SAPIENZA
UNIVERSITÀ DI ROMA

Visible Light Communication Networks for the Internet-of-Things

PhD School in Computer Science
Dipartmento di Informatica
Sapienza University of Rome, Italy

Dottorato di Ricerca in Informatica – XXXII Ciclo

Candidate

Nupur Thakker
ID number 1756408

Thesis Advisor

Prof. Chiara Petrioli

A thesis submitted in partial fulfillment of the requirements for the degree of Doctor of Philosophy in Informatica

July 2021

Thesis defended on 08 July 2021
in front of a Board of Examiners composed by:

Prof. Maurizio Bonuccelli (chairman)

Prof. Dario Catalano

Prof. Andrea Marin

Visible Light Communication Networks for the Internet-of-Things
Ph.D. thesis. Sapienza – University of Rome

© 2021 Nupur Thakker. All rights reserved

This thesis has been typeset by LaTeX and the Sapthesis class.

Version: July, 2021

Website: https://sites.google.com/di.uniroma1.it/thakker/

Author's email: thakker@di.uniroma1.it

Thesis Committee

Prof. Chiara Petrioli (First Member)
Department of Computer Science
Sapienza University of Rome, Italy

Prof. Marilena De Marsico (Second Member)
Department of Computer Science
Sapienza University of Rome, Italy

Prof. Gaia Maselli (Third Member)
Department of Computer Science
Sapienza University of Rome, Italy

External Reviewers

Prof. Laura Galluccio
Department of Electrical, Electronic and Computer Engineering
University of Catania
Catania, Italy

Prof. Francesco Restuccia
Department of Electrical and Computer Engineering
Northeastern University
Boston, USA

Dedicated to
My Grandparents

Abstract

For the last century, Radio Frequency (RF) technology has completely taken over wireless communication. Nevertheless, the ever-increasing demand and popularity of wireless embedded devices are rapidly consuming the available radio spectrum. The research communities are exploring the other parts of the electromagnetic spectrum to complement the RF frequency bandwidth with the intention to solve the RF spectrum crunch issue. Among the potentially available options, the visible spectrum is a vast and unregulated band that could be effectively used for wireless *Visible Light-based Communication* (VLC). VLC offers a critical alternative to the spectrum-challenged RF-based forms of data transmission by tapping an unutilized and unregulated frequency band. VLC also possess added advantage of being more safe and secure compare to RF technology.

With the evolution of Light Emitting Diode (LED) technology, now LEDs are more cost and energy effective, higher switching rates, and modulated at comparable rates to radio-frequency technologies. The advancement in LED technology is a significant step towards VLC.

VLC applications include wireless sensor networks, indoor localization, smart homes, vehicular networks etc. VLC systems could be used in conjunction with traditional RF-based devices to build networks with higher robustness, throughput, and spectrum efficiency. Furthermore, the seamless integration of VLC transceivers with traditional illumination devices can result in pervasive deployment. Hence, hybrid RF/VLC systems can provide an effective solution for the ubiquitous networking required by IoT deployments. Carefully designed low-cost VLC devices have the potential to enable the Internet of Things (IoT) at scale by reducing the current RF spectrum congestion, which is one of the major obstacles to the pervasiveness of the IoT. To bring the vision of illumination and communication in visible lights closer to reality, we need to identify the key challenges for reliable communication in a noisy indoor environment. However, the wide adoption of VLC devices is hindered by their current shortcomings, including low data rate, very short-range, and inability to communicate in a noisy environment.

In this regard, we propose a new software-defined VLC prototype named VuLCAN for Visible Light Communication And Networking that overcomes these limitations. VuLCAN is based on an ARM Cortex M7 core microcontroller with a fast sampling analog-to-digital converter and power-optimized Digital Signal Processing (DSP) libraries. Using BFSK modulation, the prototype achieves a data rate of 65 Kbps over a communication range of 4.5 m comparable to the state-of-the-art prototypes. VuLCAN also provides robust and reliable communications in highly illuminated environments (up to 800 lux) using only a low power Light Emitting Diode (LED), largely exceeding the capabilities of current state-of-the-art prototypes.

So far, the main focus of the research in VLC has been on the PHY layer, and less attention has been paid on the higher network layers. Studies and work on MAC/routing layers for VLC demands a new set of performance analysis tools. Simulations are useful for performance analysis in testing different setups and scenarios repetitively and optimally in terms of time and cost. We have extended the GreenCastalia simulator to implement the wireless VLC channel and VLC RADIO

layer. It is based on the Lambertian model for intensity-modulated point-to-point LED signals in indoor scenarios and the specifications of the VuLCAN prototype.

There is a need to explore more sophisticated networking approaches to unleash the potential of VLC for IoT applications and networking. There has been limited work on MAC protocols for VLC with restricted topologies like a star, broadcast, and peer-to-peer and cannot be extended easily to distributed ad-hoc networks. The MAC schemes proposed are mostly inherited directly from RF communication without much modification. Being complementary to RF, the issues in the MAC layer for VLC like directionality, hidden nodes, and blockage need to be adequately addressed. In this work, we study the limitations of RF MAC protocols when applied to VLC systems. We design and implement a novel MAC layer protocol, named Li-MAC, along with the neighbor discovery scheme considering the directional nature of VLC and its challenges.

As a summary, in this thesis, we push the envelope of existing low-end embedded VLC design towards pervasive networking and expands the range of applications of VLC for IoT.

Acknowledgments

Firstly, I would like to express my sincere gratitude to my advisor, Professor Chiara Petrioli, for her continuous support during my Ph.D. journey. She has always been a source of inspiration. Well-aware of her busy schedule, I am grateful for her patience, motivation, and immense knowledge that has guided me through this process. I have always felt more motivated and determined after each of our meetings and discussion.

I would also like to thank Professor Stefano Basagni for his enthusiasm, humbleness, and constant support throughout the Ph.D. process.

I would like to thank my thesis committee members, Professor Gaia Maselli and Professor Marilena De Marsico, as well the external reviewers of my thesis, Professor Laura Galluccio and Professor Francesco Restuccia, for generously offering their time out of their busy schedules, their guidance, and their invaluable feedback during this process.

I would also like to thank all my research group members at Senses Lab. In particular, I would like to thank Georgia Koutsandria for being a great support during the whole Ph.D. journey. Thank you, Gina, for always being there, for all the help during stressful times, helping me with Castalia, and always replying to my e-mails. Thanks to Federico Ceccarelli for being a great help and one of the nicest persons I have ever met. Thanks to Artem Ageev and Emiliano Luci for being great collaborators during our work on VulCAN. Thanks to Daniele Spaccini and Petrika Gjanci for always being an inspiration and for the idea of the chirp algorithm.

I would like to thank all the professors at IIT, Roorkee, who supported and encouraged me; Special thanks to Professor M.V. Kartikeyan and Professor Dharmendra Singh. I would also like to thank Professor Chetan Desai for his motivation and support.

A big thanks to all my friends and family who supported me and are still talking to me even when I disappeared for days or even weeks. Thank you, Uttkarsh, for all the late-night weekend discussions on exciting research ideas and for being a great friend. Thank you, Mohit, for always being just a call/ping away during all ups and downs. Thank you, Utpal, for the RF discussions and the IIT Roorkee vibe in Europe. Thank you, Dr. Hassan Elahi, for being a great friend and for all the aperitivos and desi food. Thank you, Andreja, for becoming my home in Rome. Thanks to my uncle Dr. Arvind Upadhyay for helping me navigate through the whole journey. Thanks to Nitesh Bhaiya for supporting me in this journey. Thanks to my elder sister, Natasha, for being so motivating, a great cheerleader, and for constantly checking on me. Thank you, Divyakant, for always pushing me towards betterment. Thanks to Riddhima for the help and support. Thanks to my brother Joy for being there and for always making me happy, even during stressful times.

I am beyond grateful to my mother, Vijaya Thakker, and my father, Pradeep Thakker, for their incredible support throughout this journey and value their immense sacrifices to ensure success in my life. I would not have reached my goal without the constant motivation, support, and sacrifice they have made for years at every step of my life. Thank you, mom and dad, for giving me life in the first place, for educating me to be an honest and responsible person, and for unconditional support

and encouragement to pursue my life goals. Mom and Dad, this degree is as much as yours as it is mine.

Lastly, I would not have started, continued, and completed this process without the constant encouragement and support of my partner, Abhijit Mahalunkar. Being a scientist himself, he has been my strength and support system throughout this academic pursuit and has led me towards a path full of curiosity and knowledge. I will cherish the extended discussions we had that has led to some interesting ideas and solution. I am grateful for everything he has done to make this process as easy as possible for me. Thank you, Abhijit, for holding my hand when I was not in my best moments and for celebrating with me the sweetest of my victories.

Contents

List of Figures xi

List of Tables xiii

List of Abbreviations xiv

1 Introduction 1
1.1 Visible Light Communication . . . 1
1.2 Motivations . . . 3
1.3 Contributions . . . 6
1.4 List of Publications . . . 8
1.5 Outline of the Thesis . . . 8

2 State of the Art 9
2.1 VLC Prototype Design . . . 9
2.2 VLC Channel Modeling and Simulator . . . 11
2.3 MAC Protocols for VLC . . . 14

3 VuLCAN 18
3.1 System Design Considerations . . . 20
3.1.1 Modulation . . . 20
3.1.2 Demodulation . . . 21
3.2 Hardware Design . . . 23
3.2.1 VLC Transmitter . . . 25
3.2.2 VLC Receiver . . . 26
3.3 Physical Software Defined Layer . . . 27
3.3.1 Firmware for Transmitter . . . 27
3.3.2 Firmware for Receiver . . . 28
3.4 Experimental Evaluation . . . 29
3.4.1 BER vs. Noise floor . . . 31
3.4.2 BER vs. Distance . . . 32
3.4.3 SNR evaluation . . . 34
3.4.4 Power Consumption . . . 35
3.4.5 Data Rate . . . 36
3.5 Conclusions . . . 36

4 Implementation of a Wireless Channel and Radio layer for VLC 37

4.1 PHY-LAYER Modeling and Implementation Details 38
4.2 Simulator Architecture and Parameters 40
4.3 Simulation Details 44
4.4 Conclusions 46

5 On the Design of Medium Access Control (MAC) Protocols for Visible Light Communication (VLC) Networks 47
5.1 Main Design Considerations 49
5.2 Neighbour Discovery 53
5.3 The Li-MAC PROTOCOL 56
5.3.1 DRTS (Directional Request to Send)-DCTS (Directional Clear to Send) Exchange 56
5.3.2 DATA/ACK Exchange 58
5.3.3 BUSY NODE BEACONING 60
5.4 Performance Evaluation 61
5.4.1 IEEE 802.15.7 MAC Protocol 62
5.4.2 VL-MAC MAC Protocol 62
5.4.3 Neighbour Discovery Evaluation 64
5.4.4 Simulation Scenario 68
5.4.5 Investigated Metrics 69
5.4.6 Simulation Results 70
5.5 Summary 84
5.6 Conclusions 86

6 Concluding Remarks 87

List of Figures

1.1 Thesis content 5

3.1 Bit Encoding. 21
3.2 System Architecture. 24
3.3 Input/Output Offloading. 24
3.4 VuLCAN Prototype. 25
3.5 Effect of High Pass Filter on Ambient Light. 27
3.6 Packet Frame Format 28
3.7 Pseudo Code of the Firmware for Transmission. 29
3.8 Raw Data Collected from ADC. 30
3.9 Pseudo Code of the Firmware for Reception. 31
3.10 Experimental Setup. 32
3.11 BER as a function of different parameters. 33

4.1 Representation of the model 39
4.2 Node Architecture 41
4.3 VLC Radio Layer 43

5.1 Indoor VLC Application Scenario 50
5.2 VLC node with multiple LED-PD sectors 51
5.3 Neighbour Discovery Packet Frame Format 54
5.4 VLC Scenario 57
5.5 DRTS/DCTS and BUSY Packet Frame Format 58
5.6 Timing Diagram for Li-MAC Protocol 59
5.7 DATA Packet Frame Format 60
5.8 Comparison of Total Neighbour Discovery Time for Periodic and Event-based Neighbour Discovery(ND) Approaches 66
5.9 Control packet overhead: Periodic vs. event-based neighbour discovery 67
5.10 Comparison of Packet Delivery Ratio (PDR) with Blocking probability = 20% 73
5.11 Comparison of Packet Delivery Ratio (PDR) with Blocking probability = 40% 73
5.12 Comparison of Packet Delivery Ratio (PDR) with Blocking probability = 60% 74
5.13 Comparison of Control Packet Overhead with Blocking probability = 20% 74

5.14 Comparison of Control Packet Overhead with Blocking probability = 40% 74
5.15 Comparison of Control Packet Overhead with Blocking probability = 60% 75
5.16 Comparison of Retransmission ratio with Blocking Probability = 20% 75
5.17 Comparison of Retransmission ratio with Blocking Probability = 40% 75
5.18 Comparison of Retransmission ratio with Blocking Probability = 60% 76
5.19 Comparison of Per Node Average Energy Consumption with Blocking probability = 20% 77
5.20 Comparison of Per Node Average Energy Consumption with Blocking probability = 40% 77
5.21 Comparison of Per Node Average Energy Consumption with Blocking probability = 60% 78
5.22 Comparison of Energy Efficiency with sectors = 4 for the three strategies 79
5.23 Comparison of Energy Efficiency with sectors = 15 for the three strategies 79
5.24 Per node energy consumption in networks with inter-arrival time of 1 second 81
5.25 Zoomed-in Distribution of Per node energy consumption in networks with inter-arrival time of 1 second 81
5.26 Comparison of Average Latency with Blocking probability = 20% . . 83
5.27 Comparison of Average Latency with Blocking probability = 40% . . 83
5.28 Comparison of Average Latency with Blocking probability = 60% . . 83

List of Tables

2.1 Comparison of VuLCAN with state-of-the-art related VLC devices. . 12

3.1 Electronic Components Used for the Prototype. 26
3.2 Estimated SNR. 35
3.3 Power Consumption of the Transceiver. 35

4.1 Physical Layer Parameters for Simulation 45

5.1 Simulation Parameters 70

List of Abbreviations

CDMA Code-Division Multiple Access

DSP Digital Signal Processing

FOV Field of View

IoT Internet of Things

LED Light Emitting Diode

MAC Medium Access Control

OFDM Orthogonal Frequency-Division Multiplexing

PD Photo-Diode

PHY layer Physical layer

RF Radio Frequency

Rx Receiver

TDMA Time-Division Multiple Access

Tx Transmitter

VLC Visible Light Communication

Chapter 1

Introduction

1.1 Visible Light Communication

Light is an essential element of life [58]. Light has a pivotal role in the evolution of life, be it an energy source, a medium to traverse through routes, or to communicate with each other. In ancient times, the light was used as one of the primary tools for communication and signaling [65]. The invention of the incandescent light bulb in 1879 pushed the economy for the better, and thus electrical infrastructures became part of the houses, shops, and buildings. The incandescent light bulb working is based on passing an electric current through a thin metal filament, which heats the filament until it glows and produces light [53]. The major turning point came with the invention and advancements of LED technology where electrons flow to create photons, and photons generate almost no heat [78]. LEDs also require much less energy with a very high switching speed. Thus LEDs can be modulated at rates that are comparable to RF communications. Indoor environments with lighting infrastructure deployments like malls, hospitals, and houses are, by default, suitable for the implementation of VLC communication.

For the last century, wireless communication based on the radio-frequency spec-

trum has revolutionized the way our societies work. Due to the growing demand for mobile services and applications, including smartphones, laptops, and the devices on the "Internet of Things," there is a high demand for wireless network data consumption. According to the Cisco Visual Networking Index, there will be 29.3 billion networked devices by 2023 [23]. There is a definite requirement for novel solutions to connect billions of devices. The growing popularity of wireless embedded devices drives an ever-increasing demand for wireless data, resulting in the wireless spectrum crunch. Relying on RF-based communication alone appears not to be a viable strategy anymore, as the usable RF bandwidth has become limited. Indeed, most RF bands—especially those that are license-free—are already no longer efficiently usable due to their limited capacity and to the presence of strong sources of interference.

Visible Light Communication (VLC) represents an appealing alternative to RF for networked embedded devices, such as indoor localization, Internet of Things, and vehicular networks to alleviate the bandwidth saturation problem. The visible spectrum is a wide and unregulated band that could be effectively used for wireless *Visible Light-based Communication* (VLC). VLC combines communication and illumination and is an attractive technology for a ubiquitous indoor communication system. Furthermore, VLC does not interfere with the radio spectrum, resulting in no interferences with the ongoing RF transmissions. It is also more secure; thus, it cannot be easily overheard; the eavesdropping party needs direct or indirect (through refection) line-of-sight access. The use of VLC would also reduce the health hazards caused by overexposure to RF. VLC systems could be used in conjunction with traditional RF-based devices to build networks with higher robustness, throughput, and spectrum efficiency [7].

The transmitters of VLC are light-emitting diodes (LEDs) transmitting information by modulating its light output, while the primary device of the VLC receiver is a photodiode (PD). Thanks to the advancements in the area of light-emitting diodes (LEDs), they are becoming more energy-efficient, inexpensive, readily available. It can now be used to transmit data at rates ranging from Kbps to Gbps. These significant advances enable us to move towards new pervasive smart environments

for connected devices and objects, all centered around light as a communication medium. The lighting infrastructures which are already deployed in homes, offices, and in all such places can be reused for communication purposes. Since the innate nature of light is directional, and light waves are susceptible to ambient light noises and blockages, the achievable throughput and latency could spatially fluctuate. Thus, VLC and Radio Frequency (RF), heterogeneous networks, can co-exist to take advantage of the benefits yielded by both systems to enhance communication efficiency while maintaining good reliability.

1.2 Motivations

The first step towards utilizing LEDs for illumination and communication was in the year 2000 in Japan. The researchers from Keio University in Japan proposed the use of white LEDs for building an access network [67]. Since then, there is a growing interest among researchers for VLC. The European Commission, under the EU framework Project 7 (FP7), developed optical communication to increase the RF network capacity. The project was called the Home Gigabit Access project (OMEGA) [30]. The IEEE 802.15.7 standard for VLC, which was released in 2011, was a massive step towards the real deployment and commercialization of the VLC networks [1]. The revised version of the standard was released in the year 2018 [3]. It defines physical (PHY) and medium access control (MAC) layers for visible light communication. Six physical layer modes are proposed comprising of indoor and outdoor scenarios. It focuses on the three types of network topologies, namely peer-to-peer, broadcast, and star topologies.

Nonetheless, many VLC technologies and use-cases are not properly considered and covered in the above standards. Though more thorough practical research on VLC is necessary, the entry barriers in VLC are much higher as compare to its RF technology counterparts. There are many RF solutions readily available for different protocols and bandwidths (IEEE 802.15.4, Wifi, Zigbee) along with evaluation and prototyping boards to be customized and can be used to try, test, and understand the intended research approaches. Also, on the software side, there is a lot of work

done on channel modeling and simulators, widely used for RF-based technologies. However, in VLC, there is still a strong need to do proper hardware and software development from zero even to start working on it. Due to such circumstances, so far, the work on VLC was focused more on the theoretical aspect or otherwise; a fair amount of effort and time is required to develop platforms and simulation tools for research on VLC.

The current work on VLC systems can be broadly categorized into high-end and low-end systems. High-end VLC systems use Field Programmable Gate Array (FPGA) and costly, highly sensitive light sensors [70]. They utilize sophisticated modulation techniques capable of achieving data rates up to Gbps. Most high-end systems are meant for infrastructure-based deployment, e.g., lighting fixtures as network access points [34]. High-end VLC systems are too expensive for general use in pervasive IoT devices, although they achieve higher data rates. Such systems push the limit of what is possible with VLC in terms of data rate, range, and performance. However, with the need for more sophisticated H/W and computationally heavy signal processing algorithms, they are expensive and not so usable for real-life deployments in IoT applications.

On the other hand, low-end VLC systems are based on low-cost embedded boards with limited range, and data rates [27, 41, 62, 74]. The work in this thesis comes under low-end VLC systems. The current low-end and low-cost VLC systems are limited to less than a few meter communication range with limited data rates. Since these systems have very low bandwidth requirements and mostly operate in narrow, closed spaces, they are ideal for IoT applications, including indoor localization and wireless sensor networking. However, they are highly susceptible to ambient noise, i.e., light interference like that from conventional lamps or sunlight from a window. One of the significant challenges for developing a low-end VLC system is to adopt low-cost design choices that are robust to ambient noise. The performance of the system (including BER and data rate) is immune to device placement or illumination. We attempt to fill the gap in the current state-of-the-art low-end VLC systems by proposing an embedded VLC prototype with an emphasis on finding a balance between data rate, range, power, and reliability in varied ambient noise conditions.

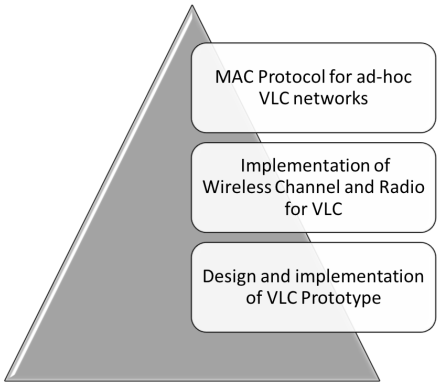

Figure 1.1. Thesis content

The content of this thesis is represented by Figure 1.1.

The majority of the proposed MAC protocols for VLC have only been studied theoretically or implemented on the packet level simulator agnostic to the wireless and radio channel for the VLC. There is a growing need for a proper simulator that could be used to study and analyze the VLC network. Some works have addressed the topics of VLC channel modeling, propagation characteristics, and simulators. However, they are mostly based on some assumptions regarding critical aspects of VLC, such as communication range, radiation pattern, power consumption, output power. It is important to implement the VLC protocols on proper network simulators taking into consideration the realistic PHY layer constraints. We have extended the GreenCastalia simulator to model the VLC channel and RADIO according to the specifications of the VuLCAN prototype [5] which we then use to evaluate the performance of network protocols.

Visible light communication is a potential alternative to RF technology for pervasive networking, but it is currently limited to point-to-point communication. Ad-hoc VLC networks can have many benefits—the directional nature of the signal results in reduced interferences and spatial reuse. There can be multiple transmissions in the same neighborhood without the destruction of the transmitted packets, which leads to the increase of the channel capacity. The MAC protocols proposed in IEEE standard 802.15.7 are mainly limited to beacon-enabled slotted and non-beacon enabled unslotted Carrier Sense Multiple Access/Collision Avoidance (CSMA/CA)

mechanism as the standard MAC protocol. It focuses on the three types of network topologies, namely peer-to-peer, broadcast, and star topologies. Due to the directional characteristics of VLC, it faces some serious challenges in an ad-hoc environment like deafness, hidden terminal issues, and blockages. This, in turn, can cause delays and packet losses. Also, neighbor discovery is a non-trivial task in VLC networks. Hence, the communication of the nodes is challenging beyond their 1-hop neighborhood. This could hinder the potential of VLC in pervasive networking. Therefore, there is a strong need for networking in low-end VLC systems. We address the above issues and propose a MAC layer protocol for low cost and low power visible light communication networks with the primary application in static indoor wireless sensor networks.

1.3 Contributions

The main focus of our work is on low-cost, low power visible light communication networking for indoor static scenarios. Our main contributions are summarized below:

- **Design and implementation of a low cost and low power embedded VLC prototype named VuLCAN.**

  We designed, built, and tested VuLCAN, an embedded VLC platform for indoor applications that is robust to ambient noise. The prototype is built using the STM32-F767ZI Nucleo board and uses low-cost and low-power COTS electronic components. We implemented DSP techniques making use of dedicated hardware, and also used I/O offloading for increased efficiency. We evaluated our system under different ambient noise conditions. Results show that it can provide a reliable and robust communication link with low BER and a data rate of up to 65 Kbps over a distance of 4.5 m in the presence of ambient light ranging from 0 to 800 lux. This contribution is detailed in chapter 3.

- **Implementation of a VLC wireless channel and RADIO model on**

Green Castalia Simulator.

We have implemented the wireless channel and RADIO layer for the VLC in the open-source Green Castalia simulator. More specifically, we obtain the actual hardware parameters from the prototype VulCAN and consider the classic Lambertian modeling of the point-to-point light signal. The PHY layer implementation is detailed in chapter 5. We also discuss the impact of the different field of view (FOV) of the LEDs and PDs on the protocol and their connectivity.

- **Design and Implementation of a MAC layer protocol named Li-MAC for VLC networking.**

  We design and implement a MAC layer protocol named Li-MAC, along with the neighbor discovery scheme, considering the directional nature of VLC and its challenges. In this work, we contribute to the research on designing a distributed asynchronous MAC protocol for VLC networks by designing, implementing, and evaluating a MAC layer protocol, namely Li-MAC (Light-MAC). To attain omni-directional communication for networking in VLC, we adopt multiple LEDs and PDs to provide 360°angle coverage. Li-MAC takes advantage of a handshaking mechanism to keep the nodes aware of ongoing communication. Particularly, during handshaking, the nodes exchange the time needed for the ongoing communication to complete and, in turn, avoid collisions and interferences without adopting strict time-division-based techniques. We compared the performance of the proposed MAC protocol, Li-MAC, with that of the state-of-the-art IEEE standard 802.15.7 MAC protocol and the multi-utility opportunistic based VL-MAC protocol with the same neighbour discovery technique, setup and under the same scenarios as for Li-MAC protocol, through extensive simulations. Results show that the proposed strategy outperforms the other two MAC protocols concerning all the considered performance metrics.

1.4 List of Publications

Papers accepted for publications and ongoing works that constitute the basis of this thesis are listed in the following.

- Artem Ageev, Emiliano Luci, Chiara Petrioli, and Nupur Thakker. "VuLCAN: A Low-cost, Low-power Embedded Visible Light Communication, And Networking Platform." In: Proceedings of the 22nd International ACM Conference on Modeling, Analysis, and Simulation of Wireless and Mobile Systems, ACM MSWIM 2019. Miami Beach, FL, USA, November 2019.
- N. Thakker, G. Koutsandria, and C. Petrioli. "On the Design of Medium Access Control (MAC) Protocols for Visible Light Communication (VLC) Networks." Under Preparation.

1.5 Outline of the Thesis

The thesis is organized as follows. Chapter 2 gives details on the current state-of-the-art works on the VLC prototypes, simulator, and MAC protocols for VLC. We present the VuLCAN prototype in Chapter 3, its motive, its complete hardware and software architecture, the reasoning behind the design choices for the hardware components, and algorithms. Chapter 4 describes the model, architecture, and implementation of the VLC module in the GreenCastalia simulator. In Chapter 5, we propose and describe the Li-MAC protocol and a comparative evaluation with state-of-the-art solutions. Finally, Chapter 6 summarizes the important conclusions derived from the thesis.

CHAPTER 2

State of the Art

2.1 VLC Prototype Design

This section aims at providing a brief review of the current state-of-the-art on low-end, embedded VLC prototypes with an emphasis on finding a balance between data rate, range, power, and reliability in varied ambient noise conditions.

Schmid et al. present one of the first low-cost LED-to-LED communication systems based on pulse position modulation (PPM), achieving a data rate of 800 bps at a distance of 2.5 m [62]. It is unclear if the prototype works in ambient light conditions. OpenVLC 1.0 is the first open-source VLC prototype based on an embedded Linux platform (BBB) adopting OOK modulation. It achieves a UDP throughput of 12.5 Kbps at a distance up to 1 m [74]. Heydariaan et al. investigate the performance of the OpenVLC platform under different experimental settings. They report that the maximum ambient light conditions supported by the system is 300 lux [36]. A two-way VLC system with a low-power single LED used as both TX and RX is presented in [47]. It achieves a data rate of 3 Kbps at a distance of a few tens of cm. The STM-32 microcontroller is used along with DC-DC booster and 9 W LED in the analog circuit to increase data rate and range performance [49]. Shine

is the first low-cost VLC platform that demonstrates distributed networking [41]. Another interesting work is the proof of concept describing how the Internet Protocol (IP) stack can operate on an LED-based VLC node [61]. However, these works do not report on tests to show resilience to ambient noise conditions. To realize effective VLC networking, robust and stable physical layer solutions are required that take into account the effect of realistic scenarios like ambient light interference.

Zhao et al. took a step forward and proposed a dedicated analog circuit to address the issue of noise cancellation in VLC receivers [82]. Similarly, Chang et al. present an attempt to remove ambient noise from the VLC circuit [17]. Both works focus on circuit designs without details about data rate and range. Wang et al. present a holistic characterization of the OpenVLC board [75]. Although their approach make the system resilient to noise by utilizing the sensing property of the LED, it shows limited sensitivity and link stability due to switching between PD and LED as the receiver antenna. Schmid et al. present a software-defined adaptive VLC network that adapts the link sensitivity based on the strength of the input signal, obtaining a data rate and range up to 5.50 Kbps and 170 cm, respectively [62, 63]. However, the paper reports the increased uncertainty in the transmission duration and throughput with this approach. Costanzo et al. propose an adaptive VLC system with a fuzzy logic-based process that changes to LEDs of different colors depending on the interfering external lights [24]. The reported data rate was limited to 125 bps at a distance of around 8 m.

In the realm of prototypes addressing the issue of ambient noise cancellation works worth citing include [31, 46, 68, 79, 80]. An adaptive ambient light cancellation receiver with BFSK modulation has been proposed that is based on OpenVLC platform [79]. The reported operating distance is limited to 50 cm with a data rate up to 3 Kbps. *Epsilon* is a VLC prototype for indoor localization. It implements BFSK modulation with channel hopping to avoid collisions of light sources in a shared light medium [46]. Zhao et al. propose a modulation technique encoding data into ultra-short, imperceptible light pulses to sustain communication even when LEDs emit extremely low luminance [68]. The work by Yin et al. concerns a prototype named *Purple VLC* that uses the technique of polarization for bidirectional communication.

The reported data rate is 50 Kbps, with a 6 m range in a single link [80]. OpenVLC 1.3 is the third version of the OpenVLC platform with a reported UDP throughput of 400 Kbps at a range of 4 m in noisy conditions [31]. However, a high-power LED working at 2.8 W is used for transmission, and the upper limit of the noise floor supported by the prototype is not clear.

Table 2.1 compares our prototype VuLCAN with current state-of-the-art embedded platforms based on their reported performance. When data was not available in the paper, we list values based on our estimations based on the described system (items marked with "*"). This birds' eye comparison clearly shows the advantages of our design and its potential to enhance the RF-based IoT landscape with VLC-based low-cost devices.

2.2 VLC Channel Modeling and Simulator

Despite the growing interest in VLC, the number of works on channel modeling, characterization, and VLC network simulators are limited.

[39] is one of the earlier works on the theoretical wireless optical channel on infrared IR channel modeling based on recursive calculation methods. It presents the characterization of infrared channels using intensity modulation with direct detection (IM/DD), including path losses and multipath responses. [66], reports the development of a MATLAB simulation tool for the indoor VLC channel characterization. It can compute the multiple bounce impulse responses of an arbitrary configuration of sources and receivers placed in a furnished office, along with all different noise contributions using the recursive algorithm. In this paper, [52], a realistic VLC channel model is presented for various indoor environments, which are based on a commercial optical and illumination design software Zemax. The work in reference cite candles is a Communication and Lighting Emulation Software (CandLES), a detailed model of the wireless VLC/lighting system and its operating environment. It studies the impact of VLC infrastructure deployments at the physical layer. There is a need for more sophisticated modeling of the electrical circuits for noise and

Table 2.1. Comparison of VuLCAN with state-of-the-art related VLC devices.

System Prototype	VuLCAN	Schmid et al. [62]	Klaver et al. [41]	Yin et al. [79]	Yin et al. [80]	Galisteo et al. [31]
Data Rate (Single Link)	65 Kbps	800 bps	1 Kbps	3 Kbps	50 Kbps	400 Kbps
Range	4.5 m	∼2 m	∼1 m	50 cm	6 m	4 m*
Modulation	BFSK	PPM	OOK	BFSK	OOK	OOK
Implementation	ARM-STM32	Atmel ATmega328P	Arduino	BBB	ARM + PRU	BBB and PRU
Ambient Noise-Floor Limit	800 lux	not reported*	not reported*	400 lux*	[Upper limit not reported]*	[Upper limit not reported]*
Antenna (TX-RX)	LED-to-PD	LED-to-LED	multiple LEDs-to-multiple PDs	LED-to-PD	multiple LEDs-to-PD*	High-Power LED-to-PD
Average Power Consumption	770 mW	∼300 mW	4 W*	∼315 mA (receiver circuitry)*	not reported*	not reported*

bandwidth performance evaluation of the transmitter and the receiver circuitry. Reference [45] provides an implementation to simulate the IEEE 802.15.7 standard PHY layer on the OMNET++ simulation tool. The models for modulation and calculation of BER are not included. All these works mentioned above mainly focus on the indoor channel model and PHY layer for visible light communication without practical validation in a real system. None of them emphasize evaluating the effects of higher layer protocols on the open-source simulator.

CamComSim [28] is the standalone Java-based simulator for the design, prototyping, and development of protocols and applications exclusively for LED-to-camera communication. [6] presents an NS3 module for VLC that is derived from existing optical wireless/VLC physical device, channel, and modulation models that can be applied to study standalone VLC systems or used to study hybrid networks. The model is validated through comparison with an actual VLC testbed implementation using GNURadio software-defined radio and USRP hardware linked to specific LED emitters and PD receivers. The modulation techniques considered are PSK and QAM. However, the receiver modeling is tied to the specific type of circuitry used for evaluation. These works are important steps towards a realistic channel model and simulation. However, they are based on some assumptions regarding critical aspects of VLC, such as communication range, radiation pattern, power consumption, output power, or more accurate only for the parameters used in the deployment. The years of research in VLC provide a rich set of models like Lambertian radiator with test-bench validation for analyzing the physical layer [6].

There is a requirement for a generic wireless and radio layer implementation on a widely used wireless network simulator to push the VLC research towards higher layers in ad-hoc wireless networking. We have implemented the wireless channel and RADIO layer for the VLC in the open-source Green Castalia simulator. More specifically, we obtain the actual hardware parameters from the prototype VulCAN [5] and consider the classic Lambertian modeling of the point-to-point light signal.

2.3 MAC Protocols for VLC

This section aims at providing a brief review of the current state-of-the-art on MAC protocols for ad-hoc VLC networks. The traditional MAC protocols designed for RF-based ad-hoc networks with omnidirectional antennas are not suitable for VLC networks. The majority of the proposed MAC protocols on VLC follow similar approaches as RF without considering the VLC characteristics and challenges. Also, they are mainly designed for point-to-point communication with a star, broadcast, and peer-to-peer topology. The MAC protocol designing for distributed ad-hoc VLC networks is still in its infancy [16].

The IEEE 802.15.7 standard for VLC presents beacon-enabled slotted and non-beacon enabled un-slotted Carrier Sense Multiple Access/ Collision Avoidance (CSMA/CA) mechanism as the standard MAC protocol [1, 3]. It focuses on three types of network topologies, namely peer-to-peer, broadcast, and star topologies.

Few works on MAC protocols for VLC are based on simple CSMA/CA-based techniques that do not entirely resolve the hidden terminal, blockage, and deafness issues [44,62,73,76]. A Carrier Sense Multiple Access/Collision Detection and Hidden Avoidance (CSMA/CD-HA) MAC protocol is proposed in [73]. It uses a single LED as an optical antenna at each transceiver with OOK modulation and manchester RLL coding. It adopts intra-frame bidirectional transmission to detect collisions and avoid hidden nodes. Schmid et al. [62] also use a simple contention-based MAC scheme, i.e., CSMA/CA protocol, to coordinate the VLC devices to access the optical medium with a single LED as the TX and RX, and the modulation adopted is PPM. In this work, they presented a full-duplex self-adaptive minimum contention window (SACW) MAC protocol for VLC star topology network systems [76]. The protocol is based on IEEE slotted 802.15.7 MAC protocol. The central coordinator node changes the minimum contention window size based on the channel's local packet arrival rate and the packet queue length. In [44], the authors address the issue of hidden node problem during up-link communication in standard IEEE 802.15.7 MAC protocol by proposing a solution based on busy-tones and centralized node with the star topology.

A full-duplex (FD)-RTS/CTS aided CSMA/CA mechanism is proposed to solve the hidden node problem in [48]. The coordinator can simultaneously receive the information and transmit the busy tone signal; hence the channel can be reserved by the RTS/CTS frame, sent before data packets for channel reservations. The targeted network topology is the star topology.

[12, 19, 25, 33] are based on multi-user access by implementing orthogonal frequency division multiplexing OFDMA on the PHY layer inspired by the RF system. This kind of system mainly came in the category of high-end systems and was employed prominently in a star topology. In [25], two multicarrier-based multiple access schemes for VLC channels, namely O-OFDM-IDMA and O-OFDMA, are compared based on simulation results. No works are supporting if ubiquitous low-cost IoT-based devices can support these types of multi-carrier schemes. [33] addresses the issue of multiple access self-organizing allocation of chunks using the busy burst protocol for an optical wireless OFDMA-TDD network deployed inside an aircraft's cabin. In [12], a heuristic-based resource allocation algorithm is proposed for the interference-aware allocation of subcarriers to receivers and power allocation for subcarriers. A framework for the system-level analysis of the downlink transmission in a DCO-OFDM-based optical attocell network is presented in [19].

CDMA based techniques [18, 20, 50, 64] are also presented in the VLC literature as a MAC technique. These mainly focus on the PHY layer coding to provide a muti-access system. Generating different codes for various links in a distributed system is a challenging task.

OWMAC protocol is based on the TDMA approach [10] and multi-sector transmission. Not many details have been provided regarding the topology and protocol. In this work [55], the authors propose enhancing slotted IEEE 802.15.7 MAC specification for VLC broadcasting service.

Hence, there is a strong demand for the design of efficient MAC protocols for distributed VLC networks. Along with this, the wireless sensor network protocol characteristics of maintaining trade-offs between throughput and latency with energy consumption, lifetime, and overall cost of the network also need to be considered.

There are MAC protocols proposed for directional antenna-based RF networks that attempt to deal with similar VLC network challenges like directionality and deafness. D-MAC [81] is one of the first MAC protocols proposed for RF networks using directional antennas. They make use of both directional and omni-directional transmissions and receptions while exchanging control and data packets. In [43], the authors exploited the directional antenna characteristics fully and, therefore, perform neighbour discovery and circular directional RTS transmission traversing in all the sectors followed by directional CTS, DATA, and ACK transmission. The nodes that receive the directional RTS, using a simple scheme of tracking the neighbors' directions, put off their transmission toward the beams that could interfere with the ongoing communication. The major difference is that there is always an option of omni-directional communication in RF networks, which eases the coordination and neighbour discovery process, whereas, in VLC networks, there is no default omni-directional communication. However, VLC MAC designs can get some intuition and inspiration from directional RF-based networks [8, 21, 43, 81].

There are a few protocols in the literature contributing to the MAC protocols for the distributed ad-hoc VLC networks. In this work [77], a hexagonal device design is proposed, and the MAC protocol is investigated for point-to-point and point-to-host topologies. They adopted carrier sense multiple access with collision avoidance (CSMA/CA) with a four-way handshaking mechanism (RTS-CTS-DATA-ACK) as the MAC solution for the point-to-point network. It is an exciting solution for the ad-hoc VLC network. Nevertheless, the work is depended on the specific hardware design and cannot be adopted so quickly. LiBeam is a cooperative beam-forming scheme for indoor visible light networking [15]. It uses multiple LEDs collaboratively to serve the same set of users, thus reducing the interference among users and hence enhancing the quality of the visible light links. However, it is mainly designed and targeted for indoor visible light down-link access network scenarios. [26] presents a software-centric VLC system in full-duplex mode with CSMA/CA and RTS-CTS as MAC solutions in mobile environment targeting mobile VLC applications like underwater communication, vehicle to vehicle communication, etc. The additional feature of the ambient light measurement (ALM) slot is incorporated in the Distributed

Coordination Function (DCF) to measure the ambient light before sending RTS. Not many details have been provided regarding the parameters chosen and algorithm implementation. Shine [41] is another crucial work that takes into consideration low-cost distributed networking for visible light communication by utilizing multiple LEDs and PDs to provide 360°coverage. It has demonstrated MAC capabilities with three nodes (toy example) using simple non-persistent CSMA. In [38], authors proposed VL-MAC, a multi-utility-based opportunistic MAC protocol for ad-hoc based VLC networks. The protocol aims at opportunistic link establishment wherein a VLN uses a utility function to identify the optimal sector that maximizes the probability of established links and promotes the full-duplex communication percentage in the network. It addresses and resolves the hidden-node and deafness issues of the VLC networks. The proposed protocol assumes full-duplex communication LED luminaries and PDs for TX and RX, respectively. The nodes in the network are required to be synchronized with each other using techniques like GPS-based clock synchronization. The evaluation of the protocol's performance is done on a packet-level simulator abstracted from the physical layer effects. However, this MAC protocol is developed with the assumption of the robust PHY layer providing bi-directional communication, which is an ideal condition, especially for low-cost VLC networks.

To the best of our knowledge, there is no work presented which takes into consideration realistic PHY channel modeling based on the VLC prototype and also implemented protocol on the same for VLC ad-hoc networking. We are trying to fill the gap in the VLC networking where we have a well-implemented VLC channel and PHY layer model and using the same to implement the distributed protocol for VLC.

CHAPTER 3

VuLCAN : A Low-cost, Low-power Embedded Visible Light Communication And Networking Platform

This chapter concerns the research on low-cost, low-power, and low-end VLC systems. Since these systems have very low bandwidth requirements and mostly operate in narrow, closed spaces, they are ideal to be used in IoT applications, including indoor localization and wireless sensor networking. In order to keep cost and complexity at bay, low-end VLC systems are based on the commercial-off-the-shelf (COTS) components, and embedded boards (e.g., BeagleBone Black) [41, 61, 74]. Light modulation techniques are generally amplitude and pulse-based because of their simplicity. However, they are highly susceptible to ambient noise, i.e., light interference like that from conventional lamps or from sunlight from a window [35, 37, 41, 74]. Indeed, one of the significant challenges for developing a low-end VLC system is to adopt low-cost design choices that are robust to ambient noise so that the performance of the system (including BER and data rate) is immune to device placement or illumination.

Several solutions have been proposed to alleviate the problem of ambient noise for low-end VLC systems [17, 24, 31, 75, 79, 82]. Hardware-based approaches focus on intensive analog circuit design, switching Light Emitting Diodes (LEDs) for photodiodes (PD) as receivers or gain control of the receiver. Modulation-based approaches adopt frequency-based or other sophisticated modulation techniques. Unfortunately, these approaches suffer from link instability, complex hardware, and high power consumption. The few prototypes that achieve acceptable robustness to ambient noise have to compromise the range (very short) and data rate (very low).

In this chapter, we contribute to the research on ambient noise-resistant, low-cost, low-power, low-end VLC by designing, developing, and testing the VuLCAN (for Visible Light Communication And Networking) system. VuLCAN takes advantage of frequency-based modulation paired with DSP techniques to obtain ambient noise cancellation while maintaining a reasonable communication range, data rate, and low power consumption. Particularly, VuLCAN employs FSK modulation and adopts the Chirp and Goertzel algorithm for signal detection and demodulation, respectively, thus following a software-defined approach [22, 59]. So far, the implementation of such techniques was mainly confined to more high-end DSP boards, FPGA-based platforms, and costly USRPs. Recent advancements in low-cost, high-performance embedded boards, like the ARM Cortex Series boards, afford us the opportunity of bridging the gap between low and high-end systems [51]. Particularly, VuLCAN is based on the ARM Cortex-M ST32 F767ZI Nucleo board, which, besides its integrated high-speed Analog-to-Digital (ADC) and Digital-to-Analog Converter (DAC), features native support for operations that are common to DSP techniques.

The contributions in this chapter are summarized as follows:

- We design, build and test a low-cost and low-power embedded VLC prototype, named VuLCAN, following a software-defined approach. VuLCAN achieves a data rate of 65 Kbps over a distance of 4.5 m with low BER (10^{-2}) under varying ambient light conditions (up to 800 lux). We implement the BFSK modulation with a sinusoid as the carrier wave.

- We provide a demodulation scheme based on using a Chirp algorithm for signal

detection and on the Goertzel algorithm along with Sliding Discrete Fourier Transform (SDFT) for signal demodulation.

- We perform an experimental evaluation to demonstrate the robustness of the system under different indoor scenarios.

The rest of the chapter is organized as follows. In Section 3.1 we describe system design considerations for VuLCAN. Sections 3.2 and 3.3 describe the hardware design and the software-defined physical layer of VuLCAN, respectively. Performance evaluation results of the proposed prototype are presented in Section 3.4. Finally, Section 3.5 concludes the chapter.

3.1 System Design Considerations

The main focus of our work is to design a system that is robust to ambient noise interference, which can be broadly divided into low frequency (50-60 Hz) and constant additive noise [37, 57]. The former is produced by lights running at the main grid frequency, while the latter mainly comes from natural lighting. This section discusses the system design choices considered for the prototype implementation. It also provides background information on the modulation, signal detection, synchronization, and demodulation techniques chosen.

3.1.1 Modulation

Binary Frequency Shift Keying (BFSK) is selected as the modulation technique using a sinusoid carrier wave [35]. BFSK, being a frequency modulation approach, offers resiliency to both types of noise identified above. The information transmitted is encoded in the variation of the intensity of the transmitted signal [37]. The instantaneous amplitude of the transmitted wave is proportional to:

$$A(t) \propto \sin(2\pi f(B(t))t + \phi) \tag{3.1}$$

$$f(s) = \begin{cases} f_0, \text{if } s = 0 \\ f_1, \text{if } s = 1, \end{cases} \tag{3.2}$$

where $f(s)$ is the frequency for symbol s and $B(t)$ is the symbol being modulated at time t and ϕ is the starting phase of the signal. The starting phase can be adjusted in order to have the transmitter power return to 0 after transmitting a symbol. Both symbols have a fixed, equal duration T_s. The bit encoding for our prototype[1] is shown in Figure 3.1. The duration of the symbol as well as the frequencies can be adapted depending on the ambient noise.

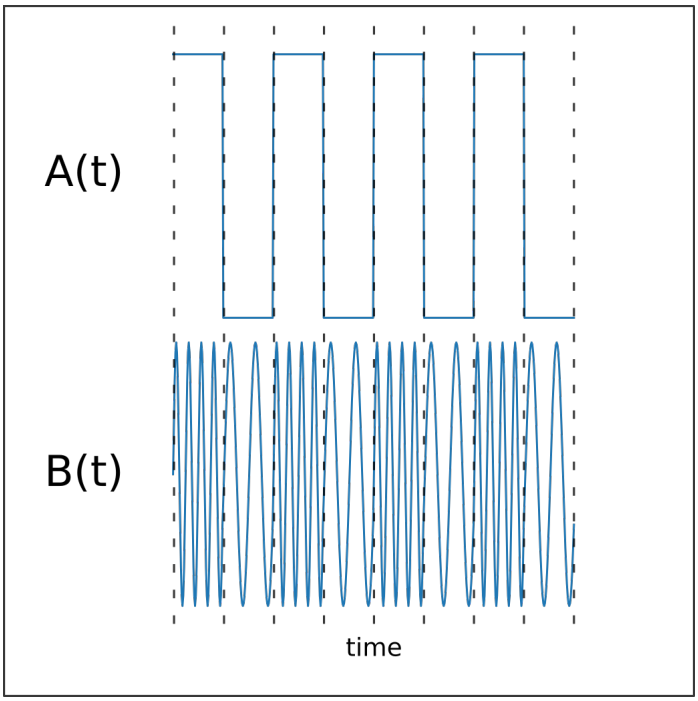

Figure 3.1. Bit Encoding.

3.1.2 Demodulation

The recovery of the digital signal from the modulated wave is comprised of two phases: signal detection and demodulation. The receiver produces a stream of values S by sampling the signal at a fixed rate. Standard DSP techniques are then used to identify and extract the frame from the stream.

[1] To ensure robust decoding, two periods per waveform are considered for each symbol.

Signal Detection

Signal detection is performed by pre-pending a chirp to the modulated data. A chirp is a linear sweep signal of finite duration between two frequencies that is represented as:

$$A(t) = A_{max} sin(2\pi(\frac{t}{2T}(f_1 - f_0) + f_0)t + \phi) \quad \text{with} \quad 0 \leq t \leq T \wedge f_1 \geq f_0 \geq 0 \tag{3.3}$$

where T is the duration of the chirp, f_0 and f_1 are the starting and final frequencies, A_{max} is the maximum amplitude of the wave and ϕ is the starting phase of the signal [14, 40]. The receiver precomputes the chirp by generating and sampling it at the same frequency as the actual signal. This will constitute the template chirp c_k, the vector of the precomputed values of the chirp of length k. The chirp is detected by performing the correlation of c_k with the values of the stream. Given the stream S, let us call $S_i : S_{i+k}$ the vector of k values of S, starting from i, and also let s_c be the index of the first value of the chirp vector in S, then

$$\begin{aligned} f(i,k) &\coloneqq (S_i : S_{i+k}) \cdot c_k \\ \arg\max_i f(i,k) &= s_c \quad \forall k, \end{aligned} \tag{3.4}$$

that is since $f(i,k)$ is the dot product of a slice of the signal with the template chirp it will trivially have its maximum when the signal aligns with the template c_k.

Signal Demodulation

The demodulation is performed by repeated application of Goertzel algorithm to the signal values [59]. This algorithm calculates a single term of the Discrete Fourier Transform (DFT) in time $\mathcal{O}(n)$. To recover an individual symbol the terms corresponding to f_0 and f_1 need to be computed and compared. Since the sampling rate of the receiver is R, then the window size, i.e., the number of samples per symbol will be $w_s = \lfloor \frac{T_s}{R} \rfloor$. This constitutes the length of the input that will be fed to Goertzel algorithm at each iteration. It follows that, in order to work, the demodulation window must be at every time aligned with a symbol in the stream.

Let $s_d = (s_c + k)$ be the index of the first value of the data in S. If $\frac{T_s}{R} \in \mathbb{Z}$ then the decoding would be trivial since the start of each symbol would always be w_s samples away from the last. However most often $\frac{T_s}{R} \notin \mathbb{Z}$, thus a technique is needed in order to adjust for slight variations in the index of the first sample of the next symbol. This is achieved by using the Sliding Discrete Fourier Transform (SDFT) algorithm [32]. It follows from the definition of DFT that if the value of a term for a window $S_i : S_{i+k}$ of values is known, then the cost to compute the same term for the window $S_{i+1} : S_{i+1+k}$ is in $\mathcal{O}(1)$. Consider a symbol with its first sample at index s_d, w.l.g. let it be the symbol for 0, call

$$\begin{aligned} m_0 &= |G((S_{s_d} : S_{s_d+k}), bin(0))| \\ m_0' &= |G((S_{s_d+1} : S_{s_d+k+1}), bin(0))|, \end{aligned} \tag{3.5}$$

where $G(\text{values}, \text{bin})$ is the Goertzel function, $\text{bin}(s)$ is the bin corresponding to the symbol frequency, and m_0, m_0' are the magnitudes of the returned vectors. If $m_0 \geq m_0'$ then the window is synchronized with the symbols, otherwise it needs to be adjusted. In this case the next symbol will be decoded starting from $s_d + 1 + w_s$. This whole procedure is repeated L times for a frame of L symbols, thus the complexity of the decoding is linear w.r.t. the length of the frame.

3.2 Hardware Design

The analog hardware design of the transceiver is fundamentally influenced by the chosen modulation technique. The transmission frequencies are constrained by the switching time of the LED, the response time of the PD, and the overall bandwidth support of the analog circuitry. Furthermore, additional constraints are imposed by the receiver characteristics, such as the ADC sampling rate as well as the processing power available for demodulation. A scheme of the system architecture is shown in Figure 3.2. The embedded board selected is a low-cost STM32-F767ZI Nucleo with integrated high-speed ADC, and DAC [51]. It is powered by an ARM Cortex-M7 processor, which is especially designed for high-performance energy-efficient

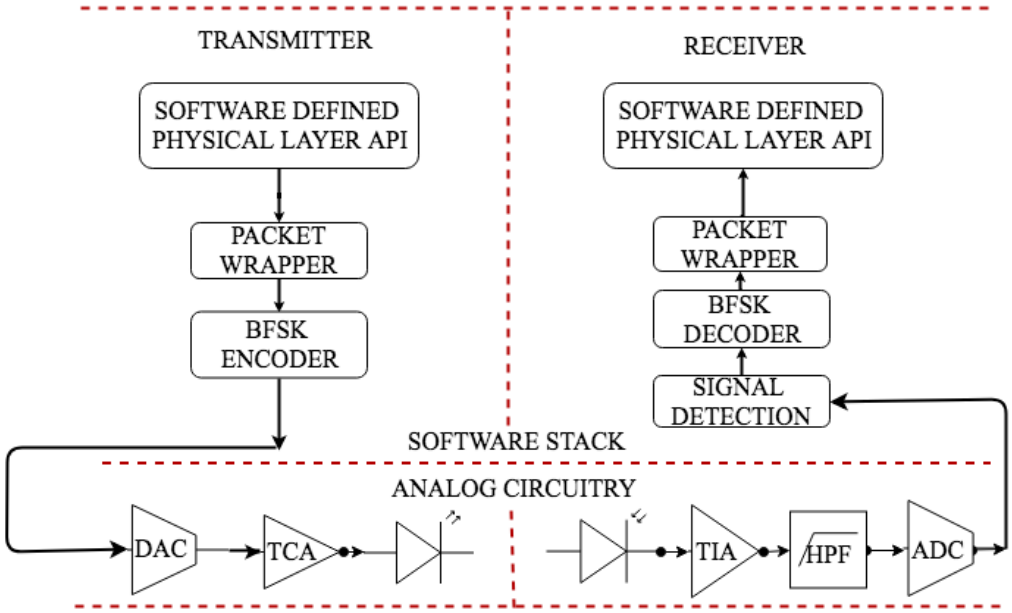

Figure 3.2. System Architecture.

applications. This CPU has a dedicated Floating Point Unit (FPU) and a Direct Memory Access (DMA) controller. The DMA, in particular, completely offloads the CPU from moving the signal data from memory to DAC (for transmission) and from ADC to memory (for reception), as shown in Figure 3.3. This way, it is possible to dedicate more computational power to the actual processing of the signal, which in turn translates into higher data rates.

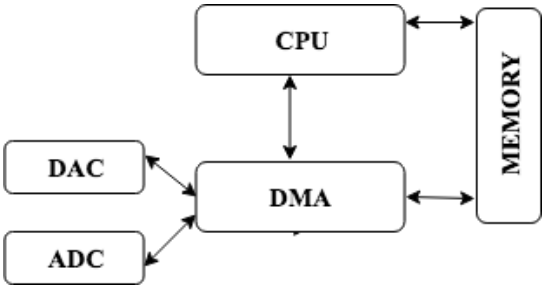

Figure 3.3. Input/Output Offloading.

The analog part of the circuitry has been realized using low-cost COTS components. The approximate cost of our VLC prototype, including the prototyping board and the analog circuitry, is around 38 euros. The hardware prototype and the list of components are shown in Figure 3.4 and Table 3.1, respectively.

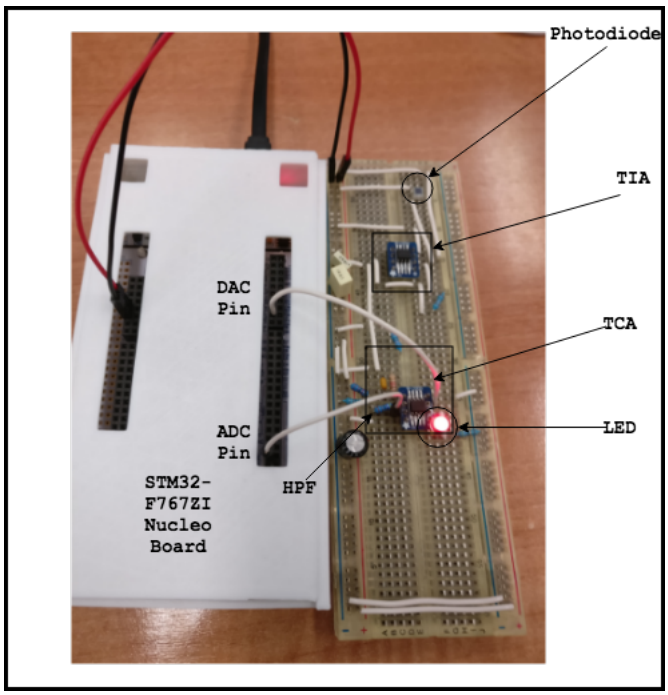

Figure 3.4. VuLCAN Prototype.

3.2.1 VLC Transmitter

The VLC transmitter (TX) consists of two parts: the Transconductance Amplifier (TCA) and the LED [37]. The TCA converts the voltage from the DAC to the current required to drive the LED, which in turn controls its intensity, and thus the instantaneous amplitude of the wave. The TCA has been selected based on its gain bandwidth product, slew rate, low noise and power consumption. The OPA2301AID has 150 MHz of unity-gain bandwidth and has an available shutdown function that reduces supply current to 5 µA when not in use is quite suitable for low-power applications. The LED has been selected based on its low power consumption, high directionality and fast switching time. The switching time of the LED determines the maximum transmission rate. The LED has a peak emission wavelength of 630 nm (red) and a field of view (FOV)[2] of 5°.

[2]Given that the PD has a wide FOV of 65°, by using multiple LEDs or wide FOV LEDs, the omnidirectional communication is possible and hence the prototype is not limited to point to point communication.

Table 3.1. Electronic Components Used for the Prototype.

#	COMPONENT NAME	PURPOSE	PRICE (€)
1.	STM32-F767ZI NUCLEO BOARD	Prototyping Board	€ 23
2.	MTE7063NK2-UR	LED	€ 6
3.	BPW34	Photodiode	€ 1
4.	OPA380AID	Transimpedance amplifier (TIA)	€ 5
5.	OPA2301AID	For Transconductance amplifier (TCA) and High pass filter (HPF)	€ 3

3.2.2 VLC Receiver

The VLC receiver (RX) consists of a Photodiode (PD), a Transimpedance Amplifier (TIA), and a High Pass Filter (HPF), as shown in Figure 3.2. The PD used for the prototype is BPW-34, which has been selected based on its fast response time, high surface area ($7\,\mathrm{mm}^2$), and good sensitivity in indoor applications. The PD is operated in photoconductive mode since it provides a better frequency response compared to the photovoltaic mode. The current flowing through the PD is linearly dependent on the irradiance measured at the surface of the PD. A TIA is used to convert this current to voltage. OPA-380 is selected as the TIA as it provides a high slew rate and 90 MHz Gain Bandwidth (GBW). It is ideally suited for high-speed photodiode applications. The gain of the TIA and hence, in turn, the feedback resistor value has to be accurately chosen, which ultimately determines the saturation limit of the VLC receiver. A high gain will give high sensitivity and thus better range, but at the same time will lead to the saturation of the TIA in high ambient light conditions. Whereas a lower gain value is more resilient to external ambient noise but will impair the reception at longer ranges[3]. The HPF is the last stage of the analog circuit, and thus its output is fed to the ADC of the Nucleo

[3] A feedback resistor value of 150K ohms is chosen empirically, which achieves the best tradeoff in our current settings.

STM32-F767ZI board. An active HPF is implemented using OPA2301AID. The choice of the cutoff frequency of the filter is influenced by the transmission and noise frequency. A high cutoff frequency will remove the ambient light noise from artificial luminaries and sunlight, as shown in Figure 3.5. However, there must be a guard band between the cutoff and the transmission frequencies to ensure that the transmission frequencies will not get filtered out.

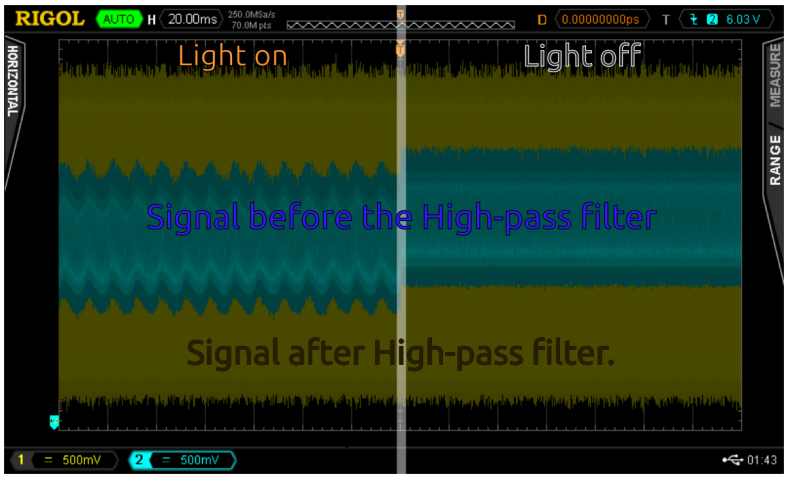

Figure 3.5. Effect of High Pass Filter on Ambient Light.

3.3 Physical Software Defined Layer

This section explains the software implementation for data encoding and modulation at the transmitter side and signal detection and decoding at the receiver side. The firmware is implemented in C language using the HAL library provided by ST-Microelectronics and CMSIS library provided by ARM. These libraries, in particular, have been optimized to make use of available FPUs to carry out common DSP operations in an efficient way.

3.3.1 Firmware for Transmitter

The Software-Defined Physical Layer exposes an API to the upper layer of the network stack to queue data for transmission as shown in Figure 3.2. When a packet

Chirp Encoding	Sync Bits	Payload
8 Symbol Periods	2 Bytes	1...64 Bytes

Figure 3.6. Packet Frame Format

gets popped from the queue, it becomes the payload for a physical frame, whose format is shown in Figure 3.6. The packet wrapper builds the physical frame by pre-pending a preamble to the data. The preamble consists of a chirp followed by two bytes of synchronization (SYNC) bits. The transmitter pre generates, samples, and stores the waveform encoding of every possible byte. A frame to be transmitted is composed by copying the preamble and the byte waveforms onto a memory buffer. The DMA unit is initialized to transfer the values from this buffer to the DAC. The rate at which the DAC consumes the buffer determines the transmitting frequency of the signal. The pseudo code of the transmission firmware is shown in Figure 3.7.

3.3.2 Firmware for Receiver

The receiver is always listening for incoming packets. The sampling of the signal is done through the combination of the onboard ADC and DMA. When the receiver is initialized, the ADC is started with a sufficiently high sampling rate and resolution (2.45 MSps and 8 bit, respectively) to ensure the best tradeoff between the conversion rate and the quantization error. The DMA is also started to copy the values from the ADC to a memory location (logically a circular buffer). The raw data collected from the ADC is shown in Figure 3.8. This constitutes the stream of values on which the CPU operates to detect and decode the frames. Every time a frame arrives and is decoded, it is put on the outgoing queue from which the upper layer can read. The pseudo code for the receiver firmware is shown in Figure 3.9.

```
def build_frame(packet):
frame.preamble = fixed_preamble
frame.payload = packet.data
return frame

def modulate(frame):
wave.chirp = generate_chirp()
for bit in bin(frame):
wave_symbol = modulate_bit(bit)
wave.data.append(wave_symbol)
return wave

def transmit(wave):
# Start the transfer from memory
# to DAC unit, returns immediately
dma_unit.mem_to_dac(wave)

def transmission_done():
transmitter_cond.signal()

while True:
packet = packet_queue.pop()
frame = build_frame(packet)
wave = modulate(frame)

transmitter_cond.wait()
transmit(wave)
```

Figure 3.7. Pseudo Code of the Firmware for Transmission.

3.4 Experimental Evaluation

We evaluate the performance of our prototype based on the following metrics: Bit Error Rate (BER) vs. Noise floor, BER vs. Distance, Estimated Signal-to-Noise-Ratio (SNR) vs. Distance, Power Consumption and Data Rate. We use a single TX-RX pair for the experiments. All results have been obtained by averaging the outcomes of 1536 packet transmission. This number of packets obtains a 95% confidence with 5% precision. The frame payloads are fixed to 8 and 16 Bytes for the experiments[4]. The experiments are repeated in various indoor scenarios covering different lighting

[4]It was observed during experiments that the signal decoding algorithm is susceptible to misalignments in the decoding window for higher payloads (54 Bytes onward), leading to higher BER which can be improved by using a forward error correction (FEC) codes.

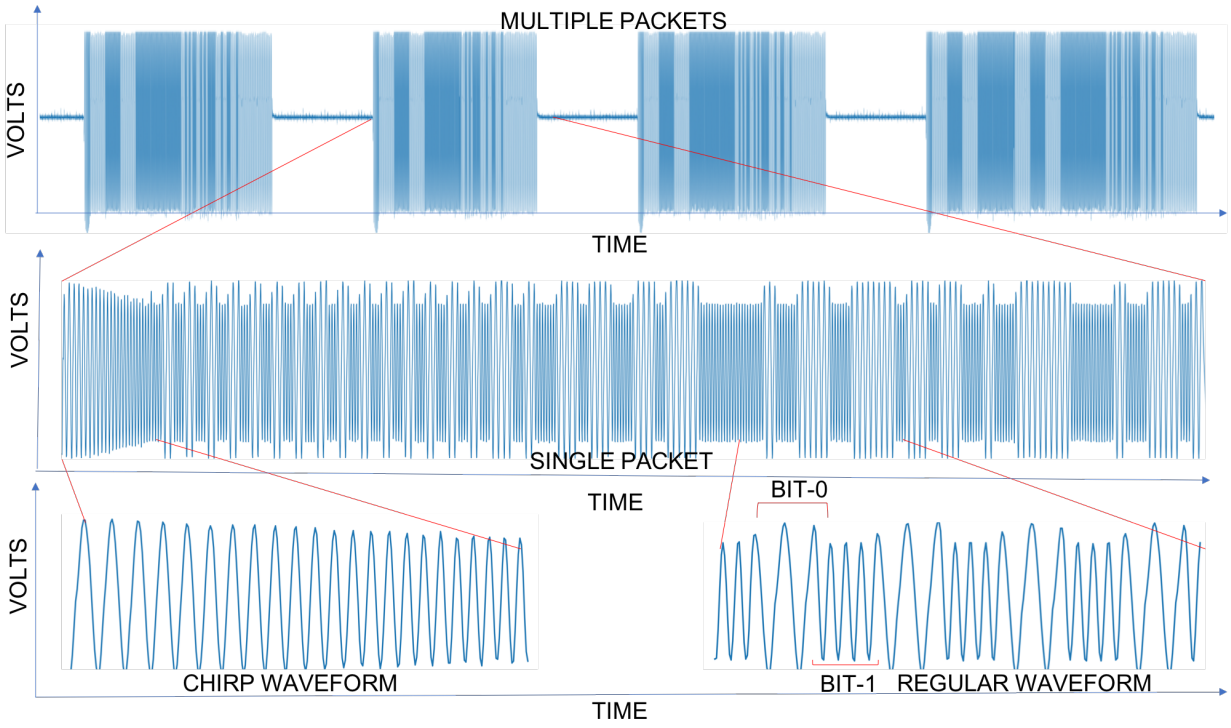

Figure 3.8. Raw Data Collected from ADC.

conditions. The illuminance under each condition is measured using the ILM-01-RSPro light meter. The experimental setup is shown in Figure 3.10. The carrier wave frequencies used for the tests are 130 KHz and 260 KHz for the symbol 0 and 1, respectively. The sampling frequency of the ADC is set to 2.45 MSps which satisfies the Nyquist sampling criteria to ensure synchronization, correct decoding, and minimal drifting with higher payloads, given the selected transmission frequencies. The cutoff frequency of the HPF is set to 80 KHz, providing an ample guard band of 50 KHz to the signal. The size of the chirp has been fixed to 114 samples per packet, which provides good signal detection performance while still being relatively fast to compute.

```
# Start the DMA unit to copy data
# from the ADC to the memory
dma_unit.adc_to_mem(circ_buffer)

while True:
# Detect the signal start using the
# chirp present in the preamble
signal_start = detect_signal_start()

# Use the preamble to correct sync
# errors and find the start of data
# symbols
data_start = sync()

while i < data_len :
next_bit = decode_symbol(
data_start + i)
data.append(next_bit)
i += symbol_len

if(detect_desync()):
resync()

frame_queue.push(data)
```

Figure 3.9. Pseudo Code of the Firmware for Reception.

3.4.1 BER vs. Noise floor

To understand the impact of ambient light on BER, we fix the distance between TX and RX to 1 m[5] and the frame payload to 8 and 16 Bytes. We have attempted to cover the whole ambient light range possible in indoor scenarios (0-1000 lux). The experiments are performed in indoor scenarios ranging from dark room to room with bright artificial lights and with open and closed windows during daytime. The BER is calculated by comparing the transmitted sequence of bits to the received bits per packet and counting the number of errors. Figure 3.11a shows that the BER, on average, is less than 2.71% for the noise floor conditions until 700 lux. Then there is a slight increase in BER and reaches to 5.28% at 800 lux noise floor. Beyond 800

[5]We have performed this experiment keeping the distance fixed, well below the maximum range, while the noise floor varies. The distance must remain constant to rule out its impact on the bit error rate.

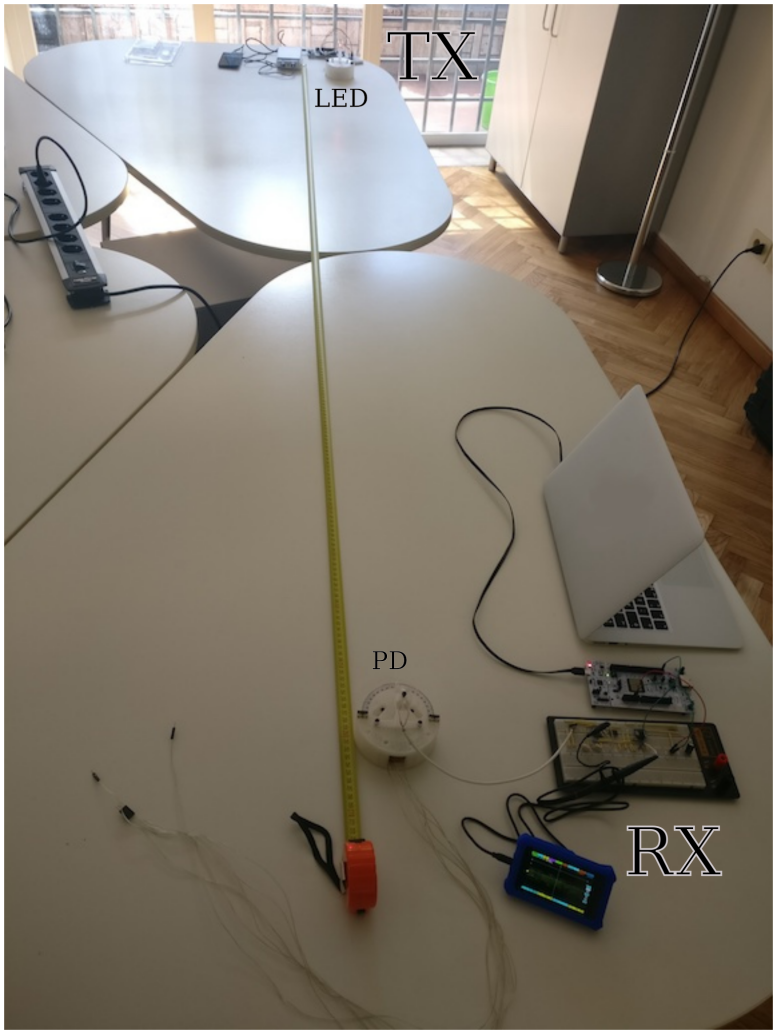

Figure 3.10. Experimental Setup.

lux, the ambient light saturates the amplifier at the receiver side and hence make it difficult to detect and decode the signals. With our current setup, the VuLCAN works well until 800 lux, which spans the entire indoor deployment. It is possible to upgrade the VuLCAN for outdoor deployments by adding highly sensitive light sensors.

3.4.2 BER vs. Distance

In this scenario, we fix the packet size to 8 and 16 Bytes. The tests are carried out in a noisy scenario of 490 lux (indoor office room with artificial lights on). The

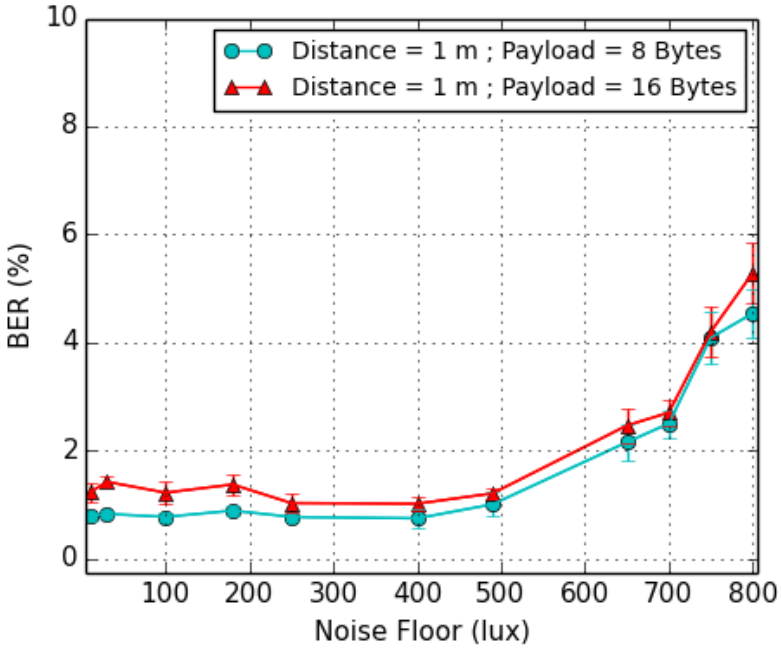

(a) BER vs. Noise Floor.

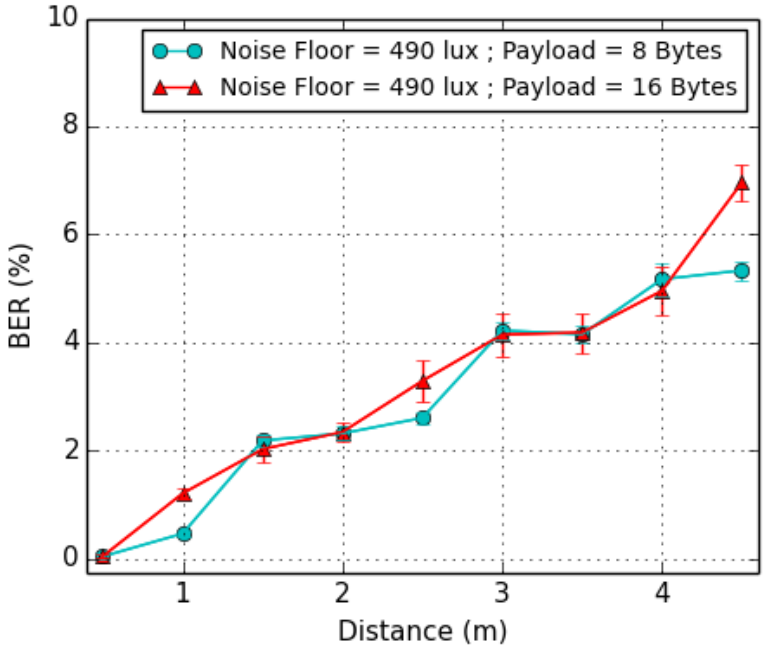

(b) BER vs. Distance.

Figure 3.11. BER as a function of different parameters.

distance between TX and RX is then varied to evaluate the range performance. In Figure 3.11b, we observe that the BER, on average, is in the order of 10^{-2} up to 4.5

m. Beyond 4.5 m, we consider the error rate to be unacceptable given the reliability requirements. The increase in BER is mainly due to extremely low signal strength at the receiver with large distances. Thus, the maximum operating range attained by VuLCAN is 4.5 m in an indoor environment. It is important to highlight that this long range is obtained with a low-power single LED as the TX. It is mainly due to the effective signal detection algorithm (chirp algorithm) that the receiver is able to detect the signal even with low signal strength. Also, the prior knowledge of the receiver about the transmitted frequencies and the DFT-based decoding make it possible to achieve reception at larger distances. In the current version, the working distance is 4.5 m, which is sufficient for indoor networking. Meanwhile, it is possible to improve the range and coverage of the VuLCAN by scaling the design with multiple LEDs or high power LEDs at the TX and with more stages of the amplifier at the RX.

3.4.3 SNR evaluation

To understand the link quality of the signal on the VLC channel effectively, the estimated Signal-to-Noise-Ratio (SNR) evaluation has been conducted with an ambient illuminance at 490 lux. The standard definition of SNR is adopted for calculation.

$$\mathrm{SNR_{dB}} = 20 \log_{10} \left(\frac{A_{signal}}{A_{noise}} \right), \tag{3.6}$$

where A_{signal} is the root mean square (RMS) voltage of signal and A_{noise} is the RMS voltage of the noise respectively. The estimate of the signal amplitude, A_{signal} is obtained from the recorded trace by fitting the already known transmitted signal waveform to the received values. The estimate of the noise, A_{noise} is calculated by subtracting the estimated signal from the recorded value. We observe from the Table 3.2 that with the frequency based modulation and demodulation technique, the prototype performs well even with extremely low SNR values.

Table 3.2. Estimated SNR.

Distance (m)	Estimated SNR (dB)
1.0	22.26
1.5	17.84
2.0	13.04
2.5	9.87
3.0	6.82
3.5	4.62
4.0	3.53
4.5	1.36

Table 3.3. Power Consumption of the Transceiver.

Components	Power Consumption (mW)
Nucleo Board (TX)	450
Nucleo Board (RX)	530 - 610
LED (MTE7063NK2-UR)	68.4
OPA 2301 (TCA and HPF)	59.5
OPA 380 (TIA)	26
Other components(resistor)	108

3.4.4 Power Consumption

The power consumption of the VuLCAN is measured as a combination of the TX and RX, as shown in Table 3.3. For each circuit component, we calculate its power by using the equation $P = VI$. The current flowing through the components is measured using a multimeter. The ARM-based Cortex-M STM32F7 Nucleo board used in our prototype is a high-performance device. Considering the aggregated

power consumption of the TX and RX, the Nucleo board consumes the biggest share ($\approx 67\%$). The LED (along with resistor) used in our prototype consumes 176.4 mW power which is nearly 4 times less than the power consumption of high power LED (1-2 W) or multiple LEDs used as a transmitter antenna. The remaining analog circuit blocks, including TCA, TIA, and HPF, consume around 85.5 mW of power.

3.4.5 Data Rate

The following factors mainly determine the data rate of the VLC prototype:

- The ADC sampling frequency
- The switching time of the LED circuitry
- The slew rate of the OP-AMP
- The response time of the PD

The effective data rate attained by VuLCAN is 65 Kbps which is comparable with the current state-of-the-art prototypes. Such a high data rate makes it suitable for a wide range of IoT scenarios.

3.5 Conclusions

We designed, built, and tested VuLCAN, an embedded VLC platform for indoor applications that is robust to ambient noise. The prototype is built using the STM32-F767ZI Nucleo board and uses low-cost and low-power COTS electronic components. We implemented DSP techniques making use of dedicated hardware, and also used I/O offloading for increased efficiency. We evaluated our system under different ambient noise conditions. Results show that it can provide a reliable and robust communication link with low BER and a data rate of up to 65 Kbps over a distance of 4.5 m in the presence of ambient light ranging from 0 to 800 lux. The prototype pushes the envelope of existing low-end embedded VLC design and expands the range of applications of VLC for IoT.

CHAPTER 4

Implementation of a Wireless Channel and Radio layer for VLC

Simulation is a critical part of designing, testing, and evaluating networking protocols and systems. Having control of the simulated environment allows us to run reproducible experiments, explore parameter spaces, and disambiguate the cause of errors. Due to the relatively long time durations and high cost needed to deploy and study wireless networks, simulations play an essential role in the development. It provides a cost and time-effective method to test the algorithms and protocols. There has been work done on the channel modeling, characterization, and VLC network simulator [6, 28, 52, 54, 60], but proper simulation tools for VLC ad-hoc networks are still missing to study and work on higher layers and full network stack.

To fill this gap, we extended the capabilities of the open-source GreenCastalia simulator to model wireless channel and RADIO layers for VLC. GreenCastalia is an extension of the Castalia simulator that is used on top of OMNeT++ to model energy-related aspects of WSNs accurately, including energy harvesting technologies [9]. Castalia is one of the widely adopted simulators for the wireless sensor networks research community, with its advanced channel and radio model for RF among other

existing simulators [11].

The rest of the chapter is organized as follows. In Section 4.1 we describe the channel model adopted for the VLC PHY-LAYER modeling. Section 4.2 describes the general structure of the VLC channel and RADIO layer extended in GreenCastalia, including a detailed description of the parameters adopted for modeling. The simulation details based on the VuLCAN prototype and which is further adopted for the implementation of the protocols, are presented in Section 4.3. Finally, Section 4.4 concludes the chapter.

4.1 PHY-LAYER Modeling and Implementation Details

This section describes the channel model that we adopted to implement wireless channel and RADIO layers for VLC. The years of research in VLC provide a rich set of models like Lambertian radiator with test-bench validation for analyzing the physical layer [4, 6]. The LED light source in VLC is approximated and modeled as a lambert radiator, which is the classic radiation model in VLC [39, 42] and has been validated on a test-bench setup [6]. There can be two types of link modeling possible in VLC, diffuse links and point-to-point links. The diffuse links are mainly possible with high-power large FOV LEDs. It suffers from high signal attenuation. The other type is the directional point-to-point links, which require multiple LEDs for 360°coverage. We have adopted directional point-to-point VLC links. This model is moderately simple and still sufficiently accurate. The model assumes that both the transmitter and receiver have a tightly constrained field of view. It does not consider optical phenomena such as diffusion that would soften these edges, making it computationally light and inexpensive, which can be useful for network scalability. The PHY layer simulates the indoor line of sight (LOS) communication between LED as a transmitter and PD as a receiver, respectively, as shown in Figure 4.1.

The main equations that govern the VLC channel are as follows :

$$m = -\frac{\ln 2}{\ln\left(\cos \phi_{1/2}\right)} \tag{4.1}$$

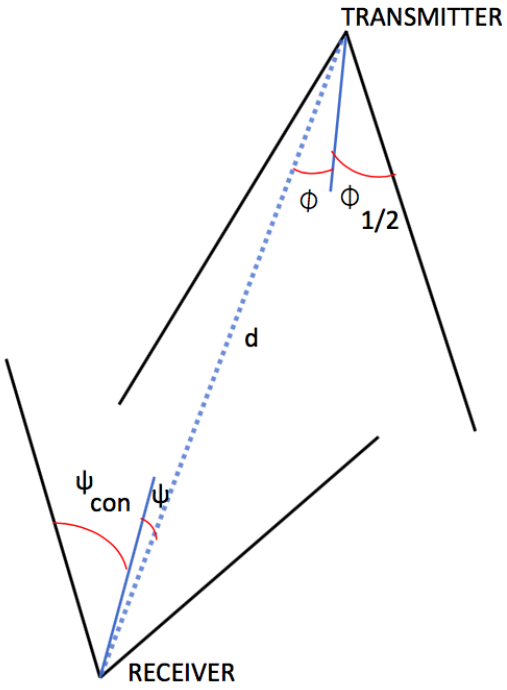

Figure 4.1. Representation of the model

where m is the lambert index, $\phi_{1/2}$ is the half power semi angle which is half of the field of view (FOV) of the LED under consideration.

$$R(\phi) = \frac{(m+1)}{2\pi}\cos^m(\phi) \tag{4.2}$$

where $R(\phi)$ is the radiation intensity, m is the lambert index of the LED light source, and ϕ is the angle between light emission direction and the normal light source.

$$H_{ref}(0) = \frac{A}{d^2}R(\phi)\cos(\psi)Rx_{Gain} \tag{4.3}$$

where $H_{ref}(0)$ is the channel gain of the VLC channel between the transmitter and receiver, A is the physical area of the photodiode, d is the distance between a transmitter and receiver,Rx_{Gain} is the gain provided by the receiver circuitry, ϕ denotes the angle between the light emission direction and the light source normal direction, and ψ is the acceptance angle at the receiver side.

$$SNR = \frac{P_r^2\gamma^2}{\sigma^2} \tag{4.4}$$

where SNR is the signal to noise ratio at the receiver end, P_r is the power received at the receiver, γ is the photodetector responsivity (A/W) and σ^2 represents the total noise variance.

The signal to noise ratio (SNR) model takes into consideration the ambient noise (noise floor).

To model data transmission, we assume a passband system realized with Intensity Modulation and Direct Detection (IM/DD) technique. The data is modulated using Binary Frequency Shift Keying (BFSK) with a sinusoidal wave, and hence flickering of the light signals can be avoided. The Bit Error Rate (BER) of BFSK in an Additive White Gaussian Noise (AWGN) channel is given as,

$$BER = \frac{1}{2}\operatorname{erfc}\sqrt{SNR/2} \tag{4.5}$$

The simulated channel model also has directivity characteristics in terms of calculating RSSI, interferences, and collisions. The occurrence of the hidden node terminal is modeled as well. Packet collisions are determined using an additive interference model by linearly summing up the effect of multiple signals simultaneously sent at the receiver. The modeling of the blockage due to obstacles in between two communication nodes is also implemented. The energy model used is also that of the proposed prototype VuLCAN extended to comprise multiple LEDs, and PDs [5].

4.2 Simulator Architecture and Parameters

This section will describe the extended architecture of the wireless VLC channel and VLC radio layer implementation. Castalia and hence also GreenCastalia are discrete event simulators and use OMNeT++ as their base foundation. OMNeT++(Objective Modular Network Testbed in C++) is an object-oriented modular discrete event network simulation framework [71]. The essential components of the OMNET++ consist of modules, messages, and gates. A simple module is a basic unit of execution, and a composite module is a group of simple modules. The modules accept messages

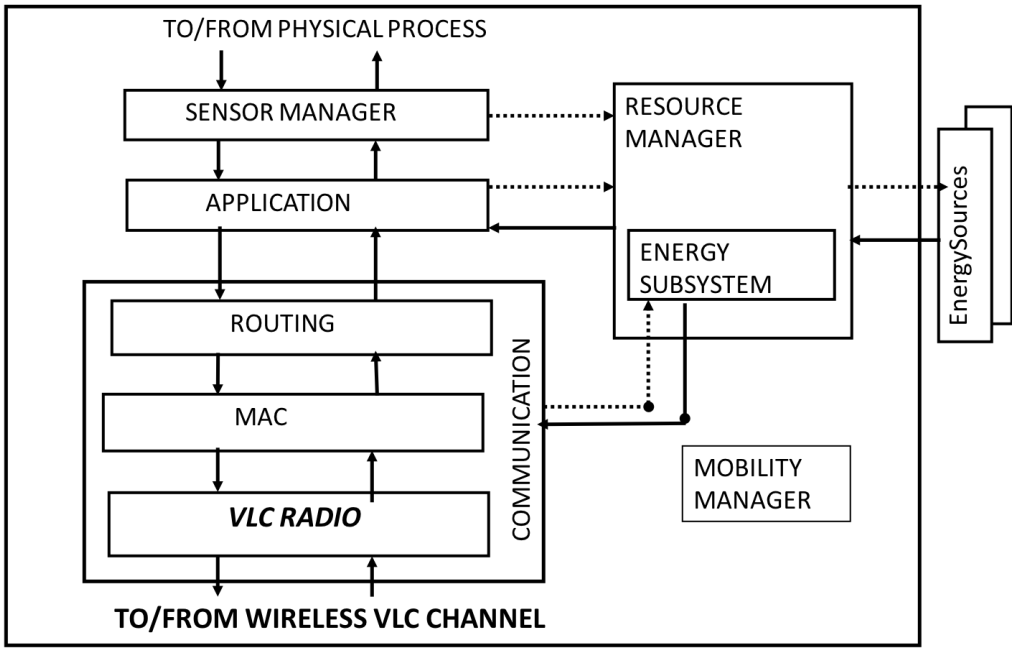

Figure 4.2. Node Architecture

from other modules or themselves, and the code execution happens according to the message. The gates are the input and output interfaces of modules. The Figure 4.2 shows a general node architecture in GreenCastalia; the boxes represent modules and compound modules. The solid arrows represent message passing, and the dashed arrows represent simple function calling.

The WIRELESS VLC CHANNEL

The wireless channel module is dedicated to carry out channel modeling in GreenCastalia. This module keeps track of the path loss and links connectivity between the nodes. We extended the RF wireless channel model of Castalia by introducing a new module, called the Wireless VLC channel, replacing the RF wireless module for what concerns the VLC channel modeling and networking. The Wireless RF and VLC channel can also be extended to be used together for hybrid RF-VLC networks. In the extended version, the wireless VLC channel models the VLC channel model, which is based on the Lambertian radiator, as described in the previous section. The main parameters for the wireless VLC channel module to calculate path loss are PD

area, Gain of the receiver, FOV of the LED, and PD and signal delivery threshold.

- PD Area : This parameter specifies the area of the photodiode used for the receiver.
- Gain of the receiver : This parameter specifies the total Gain by the receiver, including the Gain from the TIA and the filters used in the receiver. This also gives flexibility in terms of receiver designing.
- FOV of the LED and PD : This parameter determines the FOV and hence, in turn, the half intensity angles for the LED and PD used.
- Signal delivery threshold : This parameter sets a signal strength threshold that beneath it the signal will not get delivered to the receiver, which further depends on the sensitivity of the receiver.

The VLC wireless channel sends messages to the radio module. The messages carry information about the signal, such as the sector of the LED from where the signal is transmitted, modulation, bandwidth, carrier frequency, and the signal's strength in dBm. The wireless channel can calculate the signal strength received at a node using the node's path loss and transmitter power information. The option to explicitly set the path loss map, which is offered by Castalia, can also be adopted for VLC path loss. Though the main interest and focus are on indoor static scenarios, but the nodes can be modeled as mobile nodes using the mobility module feature of Castalia.

The VLC RADIO LAYER

We extend the RADIO layer of Castalia by introducing the VLC Radio features along with the primary basic features of low-cost radio used for wireless sensor networks. The VLC radio mainly consists of models of LEDs and PDs and its analog circuitry. The LED and PD are used for transmission and reception of the data, respectively. There is flexibility on the number of LEDs and PDs on the individual node, and

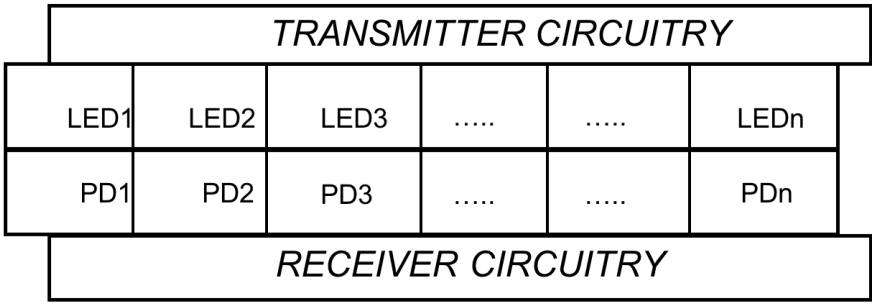

Figure 4.3. VLC Radio Layer

hence, in turn, decides the coverage of the node. In the current version, we have considered the common analog circuitry, DAC, and ADC for all the LEDs and PDS on the radio to optimize the cost and energy, which can be further extendable based on the requirements. The list of the parameters included in the VLC RADIO module is as follows : Number of Sectors of LED, Number of Sectors of PD, Responsivity, Noise Floor, Bandwidth, and Power consumption.

- Number of Sectors of LED : This parameter defines the number of LEDs on the node, which can range from 1 to any number based on the FOV of the LED to provide the coverage according to the application and requirement
- Number of Sectors of PD : Similar to the above parameter, this defines the number of PDs on the node.
- Responsivity : This parameter specifies the ratio of generated photocurrent and incident optical power, determined in the linear region of the response of the PD.
- Noise Floor : This parameter is defined as the measure of the unwanted signals (ambient light in VLC systems) and signals created from the sum of all the noise sources within a system. The noise floor level determines the lowest strength signals that can be received and is a vital characteristic of the receiver.
- Power consumption : This parameter defines the power consumption of the radio in transmission, reception, and the ideal mode.

A blockage is one of the critical characteristics of the VLC network. To simulate the blockages, we have adopted the blocking probability parameter. The blocking probability can be set to denote the chance of blockage of packet transmissions to simulate various real-life scenarios. The individual blocking probability is picked randomly for each packet transmission with reference to the selected average threshold blocking probability to simulate the varying link blockage scenario. For example, a building's crowded corridor represents high blocking probability or corners of the building with minimal obstructions denoting low blocking probability. The impact of varying blocking probability on various MAC protocols is evaluated in detail in the next chapter 5. Now provided the VLC channel and RADIO modeling modules, the VLC network upper layers stack implementation can be carried out smoothly.

4.3 Simulation Details

In this section, we focus on the main features of VuLCAN as described in chapter 3, which is used as a reference for the simulator design. This, in turn, provides practical insights that describe the LED-to-PD VLC network's communication properties. The PHY layer implementation provides flexibility in adopting any kind and the number of LEDs and PDs and varied analog circuitry. Table 4.1 represents the parameters considered in simulations. The practical use-case of the complete usage of the PHY layer for VLC in GreenCastalia is presented in the next chapter that implements MAC protocols for ad-hoc VLC networks using the same tool.

Table 4.1. Physical Layer Parameters for Simulation

Parameter	Value
Data Rate (Kbps)	65
Modulation Type	BFSK
Bits per symbol	1
Bandwidth (KHz)	600
Noise Floor (dBm)	-200
Sensitivity (dBm)	-40
Responsivity	0.52
Max range (meters)	5
Area of Photodiode (metersquare)	7.5e(-6)
Receiver Gain	15000
Field of View of LED and PD (degrees)	[24,90]
Number of LEDs and PDs on the node	[1,15]
VLC range (meters)	5
Carrier Frequency (KHz)	130
phyFrameOverhead (Bytes)	6
Feedback Resistor (Kohm)	150
Power consumption[TX mode](mW)	548.15
Power Consumption[RX mode](mW)	625.75
Power Consumption[IDEAL mode](mW)	55.75

4.4 Conclusions

By relying on the classic model of the Lambertian radiator, we implemented the wireless VLC channel and VLC RADIO module as an extension to GreenCastalia. In this way, we provided a convenient and useful way to simulate the VLC networks. The availability of such tools can offer ease to study and work on the upper layers of the system without spending time and effort on the testbed.

CHAPTER 5

On the Design of Medium Access Control (MAC) Protocols for Visible Light Communication (VLC) Networks

This chapter aims to investigate the design and implementation of a MAC protocol for VLC ad-hoc networks. VLC can be envisioned as one of the prominent technology for communication in the Internet of Things. The targeted applications include smart homes, smart cities, RF sensitive zones like airplanes and nuclear plants, defense zones, etc., where there is a strong need for ad-hoc networking.

While many MAC protocols have been proposed supporting topologies like a star, peer-to-peer, and broadcast with a centralized approach, the design and implementation of MAC protocols for ad-hoc VLC networks are still in their infancy, as described in the chapter 2.

The MAC protocols designed for RF-based ad-hoc networks with omni-directional

antennas do not work well for VLC systems. Since radio and light signals have contrasting characteristics, and hence VLC networks come with the challenge of directionality. The innate nature of the light-emitting diode (LED) and photo-diode (PD) is directional [39]. The directional transmissions in VLC in an ad-hoc environment cause some severe problems, which include deafness, increase occurrences of the hidden terminal, blockage, and the determination of neighbours' locations. Deafness is a critical challenge in directional networks, which can cause massive delays and potentially packet losses. Unlike RF radiations, visible light can get easily blocked by obstacles. Due to the specific placement, there is a possibility that the node gets blocked, which in turn results in sudden communication discontinuity. In turn, there could be a change in topology, which can impact the regular ongoing communication. Therefore, the nodes need to be sure about the availability of the neighbours for the next-hop all the time. Thus the neighbour discovery is also a non-trivial task in VLC networks. However, VLC ad-hoc networks have added advantages as well. The directional nature of the signal results in reduced interferences and spatial reuse. There can be multiple transmissions in the same neighbourhood without the destruction of the transmitted packets, which leads to the increase of the channel capacity.

Hence, there is a need to design efficient MAC protocols for VLC ad-hoc networks for low-end systems. The protocols should also consider trade-offs and challenges of low-end wireless networking in terms of throughput, latency, energy consumption, lifetime, and overall cost of the network.

This chapter describes our contribution to the research on the design of a MAC protocol for an ad-hoc VLC network. We designed and implemented a distributed asynchronous MAC protocol named as Li-MAC (Light-MAC) protocol. To attain omni-directional communication for networking in VLC, we adopt multiple LEDs and PDs to provide 360 °angle coverage. Li-MAC protocol takes advantage of the handshaking mechanism to keep the nodes aware of ongoing communication. Notably, during handshaking, it exchanges the time needed for the ongoing communication to complete and, in turn, avoids collisions and interferences without adopting strict time-division-based techniques. The proposed Li-MAC protocol is implemented and

evaluated on Green Castalia with VLC channel and RADIO as the PHY layer as described in the chapter 4.

The contributions in this chapter are summarized as follows:

- We design and implement a MAC layer protocol, named Li-MAC, along with the neighbour discovery scheme taking into consideration the directional nature of VLC and its challenges.
- We compared the performance of the proposed MAC protocol, Li-MAC, with that of the state-of-the-art IEEE standard 802.15.7 MAC protocol and multi-utility opportunistic VL-MAC protocol, through extensive simulations. Results show that the proposed strategy outperforms the other two MAC protocols concerning all the considered performance metrics.
- We further shed light on the impact of the different field of view (FOV) of the LEDs and PDs selected for the VLC node on the VLC connectivity and the protocols.

The rest of the chapter is organized as follows. In Section 5.1 we describe the system design considerations for the proposed Li-MAC protocol. The neighbour discovery techniques adopted are described in section 5.2. Section 5.3 describes the Li-MAC protocol in detail. Performance evaluation results of the neighbour discovery techniques and the proposed protocol, along with comparisons with two MAC protocols, IEEE 802.15.7 CSMA/CA and VL-MAC, are presented in Section 5.4. Section 5.5 presents a comparison summary of all three protocols. Finally, section 5.6 concludes the chapter.

5.1 Main Design Considerations

We intend to propose a MAC layer protocol for low cost, and low power static ad-hoc VLC networks with the primary application in indoor wireless sensor networks as shown in Figure 5.1. The significant challenges which need to be addressed in the VLC networks are directionality, deafness, and blockage. A static indoor network

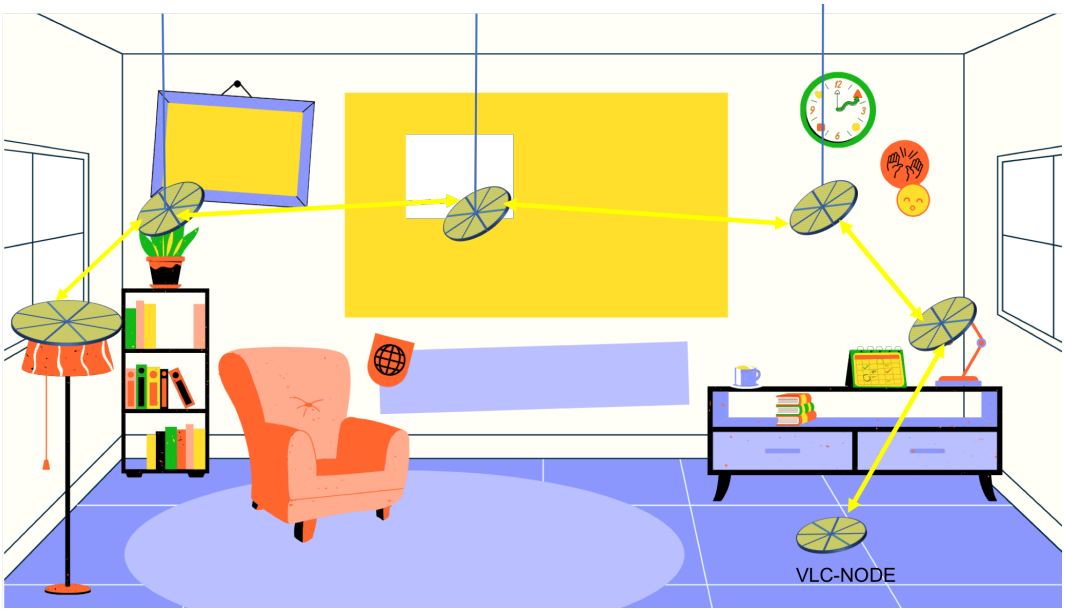

Figure 5.1. Indoor VLC Application Scenario

is considered in the design of the MAC protocol. All the nodes in the network are assumed to be capable of bi-directional half-duplex communication. Each node is assumed to be aware of its location in terms of device coordinates. Based on the above design assumptions and hence the system's limits, we consider the following design choices for the proposed MAC protocol.

- Every VLC node comprises multiple LEDs and PDs divided into sectors to mitigate the challenge of deafness and directionality. Let us consider the number of sectors as M; hence M LEDs and PDs provide omni-directional (360 °) coverage in an indoor static setting, as shown in 5.2 . Therefore, each sector on a node consists of a single LED and PD.

- We consider one digital to analog converter (DAC), one analog to digital converter (ADC), and a single-core processing unit per node. Hence, the node can process only one packet at any given point in time, maintaining the hardware requirements and the cost to its minimum.

- Since we assume bi-directional half-duplex communication, the node can either transmit or receive at any given point in each sector. The placement of LEDs

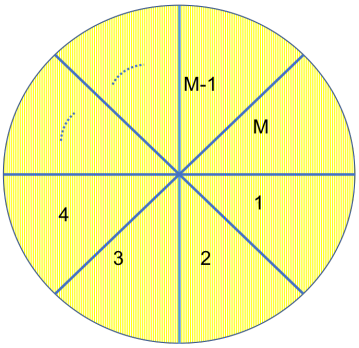

Figure 5.2. VLC node with multiple LED-PD sectors

and PDs on the node will also play a huge role. Therefore, we need to be careful about the self-interferences between LEDs and PDs on the same node, which could be among the adjacent or the same sectors. Also, only one LED will be ON (hence transmitting) for every individual node at any given point in time.

- The following states are considered for any node in the network:
  - IDLE state: where node listens using PDs in all the sectors in receiver mode. Considering an extremely low-power receiver, it can listen with all its sectors ON during listening mode.
  - TX state: where a node can transmit its signal through any one of the M sectors.
  - RX state: where a node is waiting for the packet reception. The node cannot transmit when it is receiving.
- An efficient and straightforward neighbour discovery mechanism is required to identify the neighbour location and thus the sector and orientation of the neighbouring node. This information will be useful for directional transmissions. The scheme must exchange short information between nodes. In indoor static networks, initially, it is performed before the node starts transmitting the data packets. However, there can be a provision for repeating the neighbour discovery depending on the topology and traffic in the network.

- An identifier for the sector through which the packet is transmitted along with the location coordinates of the node is embedded with every neighbour discovery packet in the communication. Based on the packets received, each node maintains a mapping in the neighbour table that describes the node id, location coordinates, and the neighbour node's LED sector from which the packet has been transmitted. Also, the sector number of the PD through which the node has received the specific packet is recorded in the table. Eventually, after the neighbour discovery phase, all the nodes in the network are aware of their respective neighbour nodes with their corresponding ids, location coordinates, and sectors for communication.

- In scenarios where the FOV of the LED is not equal to the FOV of the PD, and thus there is a possibility of the node receiving beacon/signals in multiple sectors (mostly adjacent sectors) from the same node simultaneously. The sector that receives the signal at the earliest among all the receiving sectors is considered for further communication, given the node's limited processing hardware.

- A proper handshaking mechanism is adopted for data transmission to deal mainly with the classic hidden node problem and blockage issues in directional communication.

- Availability of system-wide synchronization among nodes might not be so apt for the sensor networks where the topology and the number of nodes are flexible and can increase or decrease based on the requirements and the application scenarios. Thus time-division multiplexing access (TDMA) based MAC protocol achieving network-wide synchronization is considered not so practical for ad-hoc VLC networks. So the proposed protocol will have minimum synchronization requirements among the nodes to make the network as flexible as possible.

- The control packets and data packets exchange operate on the same wavelength LED and PD to keep the hardware requirements at a minimum.

5.2 Neighbour Discovery

The neighbour discovery is a critical step in VLC networks since it is more challenging in a directional wireless network to discover neighbour nodes than its omni-directional counterpart [13, 29, 56, 72]. For example, the omni-directional RF networks can perform neighbour discovery with a broadcast exchange of packets that can reach all nodes within the transmission range. Whereas in directional networks, for instance, in VLC networks, the limited radial range of the directional antenna's beam-width (narrow FOV of LED and PD) requires the neighbour discovery scheme to be repeatedly performed in a different direction to cover the complete 360-degree coverage. The neighbour discovery might need to be repeated in VLC networks amid the ongoing data exchanges to overcome blockage or deafness in a specific direction. Thus there is a requirement of redesigning and implementing neighbour discovery techniques for the VLC networks. Since the focus of the proposed protocol is on distributed asynchronous approaches, we have targeted the neighbour discovery design, which involves a simple asynchronous distributed approach.

The neighbour discovery is performed in two phases: the initial neighbour discovery along with the neighbour table set up and then the neighbour table maintenance. The first phase is accomplished at the beginning of a network setup. Every node maintains a neighbour table with the records from every other node it has heard. Initially, the table is empty and is updated with the reception of the neighbour discovery packets. We assume that each node is aware of its node ID and location coordinates. During the neighbour discovery phase, each node transmits neighbour discovery packets sequentially through all its sectors. In the neighbour discovery packet, the transmitter includes a number, which indicates the LED sector through which the packet was transmitted along with its node ID and the location coordinates as shown in Figure 5.3. In this manner, with the reception of a packet, a node can update the sector and location information of the corresponding neighbour. The neighbour discovery process, in the beginning, is serialized among all the nodes. The timer dedicated to each node's neighbour discovery gets triggered according to the self-node ID. The timer is also set to consider the slight drift in the clock

Source	Source LED Sector	Source Location Coordinates
4 Bytes	1...maxSectors(M)	6 Bytes

Figure 5.3. Neighbour Discovery Packet Frame Format

settings of the nodes. Therefore, each node can perform neighbour discovery in a limited time and reliably attain the neighbour node information without collisions and interference issues.

With every neighbour discovery packet received, the node maintains the following information in its neighbour table:

- Neighbour ID (the node from which it has received a packet).
- Location Coordinates (of the source node).
- The LED sector (the LED sector through which the neighbour node has sent the discovery packet).
- The PD sector (the PD sector from which the node has received the packet).

In this way, each node maintains pairs of LED-PD sectors that are used for transmission and reception.

A round of neighbour discovery is completed when a node is switched to all of its sectors for neighbor discovery. The number of neighbour discovery rounds per node can be decided based on the blocking probability scenario. With higher blockages, more rounds would be required as compared to low blocking probability scenarios. The time taken by an individual node for the neighbour discovery T_n depends on the number of neighbour discovery rounds and the number of sectors on the node. With the increase in sectors, hence with the lower FOVs of LEDs and PDs, the discovery time will increase. The time spent by a single node on the neighbour discovery is

given by,

$$\begin{aligned} T_n = &(\text{Number of sectors}) * (\text{Number of rounds}) \\ &* (\text{Tx time of the individual discovery packet}) \\ &+ (\text{Number of rounds}) * (\text{Time duration between the rounds}) \end{aligned} \quad (5.1)$$

The whole network discovery time mainly depends on the total number of nodes in the network, along with the number of sectors on the node and time duration between the rounds. The network discovery time T_N is given by,

$$T_N = (\text{Number of nodes}) * (T_n) \quad (5.2)$$

Once the initial neighbour discovery phase is over, further neighbour discovery and maintenance can be performed either by adopting **Periodic neighbour discovery** or **Event based neighbour discovery** approach.

- **Periodic Neighbour Discovery**

  In Periodic neighbour discovery, after every fixed periodic time interval, all the nodes in the network repeat the same neighbour discovery procedure serially. Due to the limited range and directionality in VLC, there is an added advantage of spatial reuse. Hence, there are fewer chances of a collision amid the ongoing data transmission compared to omni-directional networks. Although the serialized periodic approach offers reliability in neighbour discovery, the discovery time linearly increases with the increase in nodes and sectors on the node.

- **Event-Based Neighbour Discovery**

  Since the assumed scenario is the static indoor network, there is also a possibility that not all nodes in the network require a neighbour discovery periodically. Thus, we can save on control packet overheads and energy consumption incurred due to periodic neighbor discovery rounds. In that case, **Event based neighbour discovery** can be adopted to discover neighbour nodes amid the ongoing data transmission. With this approach, the neighbour discovery and

maintenance are made locally by the individual node based on the triggering event. For instance, as an event, we can consider the node going through consecutive data packet drops three times in a row, triggering the neighbour discovery round and thus update the neighbour table. The nodes receiving the discovery packets sent a discovery acknowledgement packet to the node from where it has received the discovery packet. However, they deter from starting their neighbour discovery during that period to lower the chances of collisions and to have minor disturbance on the ongoing data transmissions. The choice of the event can vary depending on the application and scenario.

5.3 The Li-MAC PROTOCOL

The design considerations (assumptions and choices) mentioned in section 5.1 constitute the main guideline for the principles that govern the design of a distributed asynchronous MAC protocol for ad-hoc VLC network, named as **Li-MAC (Light-MAC) protocol**. Li-MAC protocol is an asynchronous protocol handling VLC challenges of hidden nodes, deafness, and blockages. It utilizes a single channel for data and control packet exchanges. It works on handshaking and virtual carrier sensing mechanisms to deal with **hidden-terminal** and directionality and ultimately addresses the low-end VLC ad-hoc networking challenges with the asynchronous approach [2].

Let there be N nodes in the VLC networks. The next-hop for the source node is selected as any of its neighbour node that is closer to the node indicating the destination and provides forward progress, as shown in the Figure 5.4.

5.3.1 DRTS (Directional Request to Send)-DCTS (Directional Clear to Send) Exchange

When a node has a DATA packet to transmit, it initiates the channel sensing. If the channel is found CLEAR, it transmits a DRTS frame in the chosen neighbour node's direction through the specific sector. The DRTS frame is as shown in Figure 5.5.

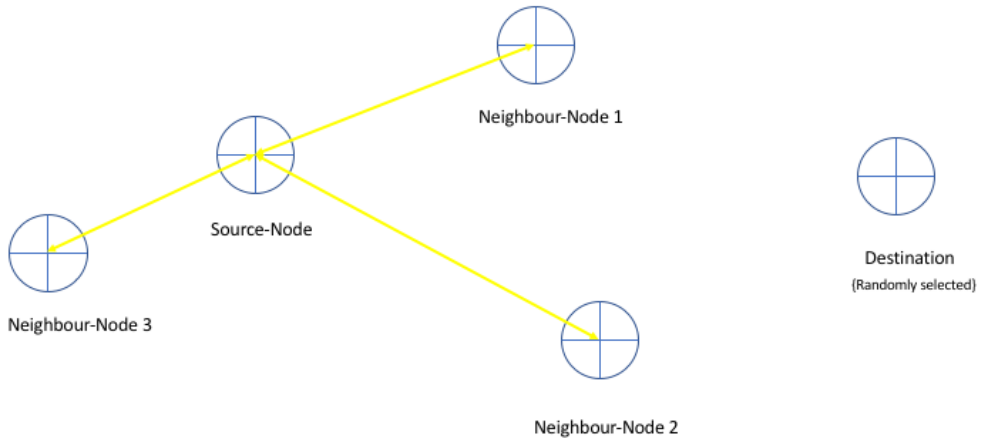

Figure 5.4. VLC Scenario

Along with the necessary information, the frame also contains information about the duration of the pending handshake in the variable called network allocation vector (NAV) measured in time (milliseconds). Therefore, by utilizing NAV information, all the nodes that receive this DRTS packet and are not the targetted neighbour node avoid starting a new transmission during this period, minimizing the interference and collisions. This adopted mechanism is called Virtual Carrier Sensing, which is inspired by the IEEE 802.11 standard [2]. In the virtual carrier sensing mechanism, every node maintains a Network Allocation Vector (NAV). NAV is initially equal to zero. When a node hears one of the two frames (DRTS and DCTS), it updates its NAV with the pending handshake duration. If NAV is a positive number, a decrement counter starts, preventing itself from transmitting until its NAV reaches zero again. Thus, every node performs a virtual Carrier Sensing to enhance the resistance of the protocol against collisions.

On the receiving side, if the selected neighbour node receives a DRTS frame, it replies with a DCTS frame and waits for the data packet reception. The DCTS packet also contains information about the remaining pending handshake duration, similar to the DRTS frame. Therefore all the other neighbouring nodes receiving DCTS and which are not involved in ongoing communication avoid a new transmission for

Source	Destination	Source LED Sector	NAV
4 Bytes	4 Bytes	1...maxSectors	ms

Figure 5.5. DRTS/DCTS and BUSY Packet Frame Format

the period contained in NAV. If the channel is found BUSY, the node backs off for a random backoff period based on IEEE 802.15.7 standard [3] and then attempts again. It repeats this process at a maximum of K times.

Nevertheless, there could be a possibility that after sensing the channel CLEAR and sending the DRTS, the source node is unable to receive a DCTS from the selected neighbour node. The reason can be **blockages** due to some object's placement, or some passerby, etc., between the source and the neighbour node, which creates an obstacle for communication. In that case, the source node deals with the blockage in the following manner. The node refers to the neighbour table again. It attempts to forward the same packet to a different neighbour node, which lies in the same forward direction as the previous neighbour node, but it could be present in another sector of a source node. Lastly, even after a certain number of tries through different neighbour nodes present in the neighbour table, which provides the forward progress to the destination, if the source node is unable to receive any response, it drops that packet and returns to the default mode.

5.3.2 DATA/ACK Exchange

After the successful DRTS-DCTS exchange among the source and the finally selected neighbour node, the sender node transmits the DATA packet to the neighbour node. Once the DATA packet is sent, the node waits for the acknowledgement (ACK) packet from the receiving node.

After the reception of the DATA packet, the neighbour node transmits an ACK to the source node and goes back to IDLE mode. Upon reception of the ACK packet, the source node also goes back to the IDLE state. If the source node does not receive an ACK within a predefined time, it re-transmits the DATA packet to the neighbour

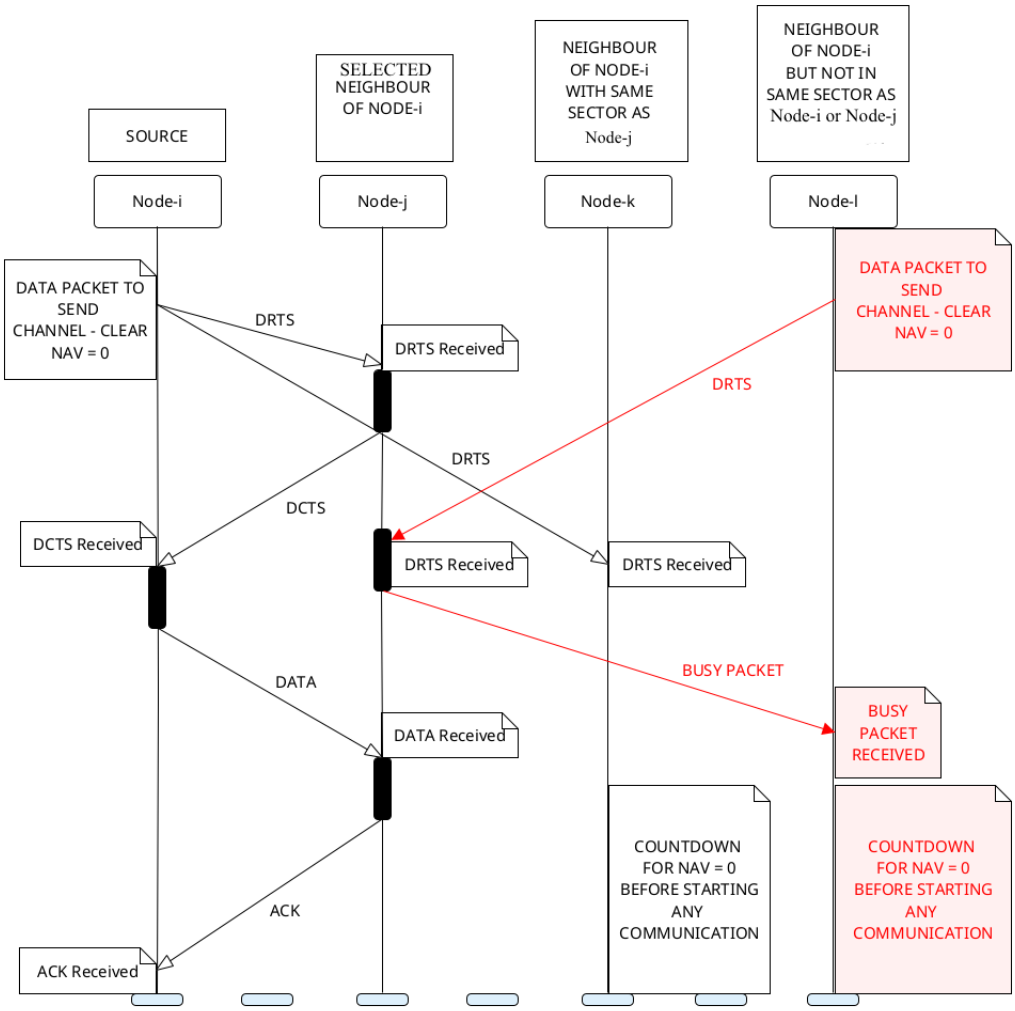

Figure 5.6. Timing Diagram for Li-MAC Protocol

Source	Dest.	LEDs	PDs	PAYLOAD
4 Bytes	4 Bytes	1 Byte	1 Byte	32 Bytes

Figure 5.7. DATA Packet Frame Format

node up to a number of N tries. The DATA packet is dropped if all re-transmission attempts (N) fail. The timing diagram explaining the handshaking mechanism in the Li-MAC protocol is shown in Figure 5.6. The frame format of the data packet is shown in Figure 5.7.

5.3.3 BUSY NODE BEACONING

The exchange of DRTS/DCTS packets will be overheard by all other neighbouring nodes, which fall in the same sectors of either source or targetted destination node of the ongoing packet exchanges. However, some neighbouring nodes could not fall in the common sectors of ongoing communication. If any of these nodes communicate with the currently active source or destination node. In that case, it will not result in a collision with the current packet exchanges since it does not transmit in the common sectors. However, finding the targetted node busy with the ongoing communication (due to limited resources of DAC, ADC, and CPU), there is a possibility of **deafness**. Deafness is caused when a transmitter fails to communicate to its intended receiver because the receiver is engaged in communication towards a sectorial direction away from the transmitter. Suppose this transmitter node is not timely informed about the ongoing communication. In that case, it might exhaust all its packet transmissions and re-transmissions and eventually drop the packet and assume congestion as a cause of failure.

The busy-tone signaling is a commonly adopted method to deal with deafness [69]. In this, the node currently busy with ongoing transmission transmits a busy tone in the out of band channel to inform the other nodes of the ongoing transmission. However, this approach is heavy on sensor networks' energy, circuit complexity and demands additional hardware on the node. Also, just a simple tone generating and

receiving circuitry is insufficient to precisely detect from which node the tone is being heard, leading to additional algorithms and circuitry requirements.

To resolve the deafness issue, we adopted a slightly different approach. When a node receives a DRTS packet amid an ongoing communication exchange from some other neighbouring node in another sector. Also, provided that during that time instance, it is not involved in any processing and can receive and process the DRTS packet(DRTS packet being a control packet is not that large and thus can be processed quickly). Therefore, the node sends a BUSY NODE BEACON PACKET to the neighbour node (from where it has received a DRTS packet) in another sector. The BUSY NODE BEACON PACKET consists of the source, destination, and the NAV value of the pending handshake as shown in the Figure 5.5. In this manner, the transmitter node is informed about the ongoing transmission. Thus, after receiving the BUSY NODE BEACON PACKET, the transmitter node can stop further transmission and wait for a specific time according to the NAV value in the packet received before attempting another data transmission as shown in Figure 5.6. Hence this technique reduces deafness in the directional VLC network.

5.4 Performance Evaluation

The effectiveness of the proposed MAC protocol Li-MAC is evaluated by simulation-based experiments. We compare its performance with two protocols, the standard IEEE 802.15.7 MAC protocol and the VL-MAC protocol using the same neighbour discovery technique, setup, and under the same scenarios as for the Li-MAC protocol. All three protocols are implemented in the extended version of the open-source simulator GreenCastalia that takes into consideration the wireless channel model and the radio layer for VLC as described in chapter 4. We start by providing a summary of the standard IEEE 802.15.7 MAC protocol and the VL-MAC protocol. We then describe the neighbour discovery performance evaluation, the considered simulation scenarios, the investigated metrics for all protocols, followed by the simulation results.

5.4.1 IEEE 802.15.7 MAC Protocol

The IEEE 802.15.7 standard for VLC presents beacon-enabled slotted and non-beacon enabled un-slotted Carrier Sense Multiple Access/ Collision Avoidance (CSMA/CA) mechanism as the standard MAC protocol [1,3]. It focuses on three types of network topologies, namely peer-to-peer, broadcast, and star topologies. Out of the above random access methods [3], the non-beacon enabled un-slotted CSMA/CA MAC protocol is suitable for the low-end VLC ad-hoc networks as it does not require any centralized coordinator control approach. In this random access protocol, every device is allowed to communicate with every other device within its range and sector coverage area.

Every time a device has a data frame to transmit, it selects a neighbour node from the neighbour table, which provides forward progress to the destination. It then waits for a random backoff period and performs the carrier sensing on the channel. If the channel is found CLEAR, the node transmits its frame of data. If the channel is BUSY, the node waits for another random period before re-accessing the channel. If, after a specific number of tries K, the node cannot access the channel, it drops that packet and returns to the default mode. Otherwise, once the targetted neighbour node receives the DATA packet, it transmits an ACK without using a random access mechanism. If the source node does not receive an ACK after some period, it assumes that the transmission was unsuccessful. The node then re-transmits the DATA packet to the neighbour node. The number of retransmissions (N) is based on the IEEE 802.15.7 standard. The data packet is dropped if all retransmission attempts fail.

This protocol is simple and thus incurred less energy and latency. However, it is unable to handle the VLC challenges for low-end ad-hoc networks. There is no provision to handle blockage or directionality in the network.

5.4.2 VL-MAC MAC Protocol

The VL-MAC protocol proposes the concept of opportunistic link establishment to deal with hidden nodes, deafness, and blockage in ad-hoc VLC networking [38]. In

the VL-MAC protocol, the nodes have two operational modes, S-IDLE(Synchronous Idle) and T/R (Transceiving State). In S-IDLE, following a fixed sector pattern, nodes sequentially listen in every sector. For every DATA packet transmission, a node uses a utility function to select the optimal sector corresponding to its maximum $Uini(s)$ that maximizes the probability of establishing a link. The utility function is based on the forward distance and the data packet backlog. Then it waits for a random back-off period depending on its $Uini(s)$ and performs the carrier sensing on the channel. It then broadcasts an Availability Request (ART) packet if the channel is found CLEAR within the sector duration's ART transmission period. The ART packet contains information related to the source node, such as node ID, location, backlog length of the buffer considered for the given sector, and channel state. All the neighbour nodes which receive the ART packet will switch to T/R state and calculate their respective acceptor's utility function, $Uacp(i)$, using information from all the ART packets received during the sector duration. The acceptor utility function is also based on maximum differential backlog, channel capacity, and forward progress from both directions. Accordingly, the acceptor chooses one initiator (source node) to which it wants to provide access for the data exchange. Moreover, it transmits an Availability Confirmation (ACN) packet to the selected source node.

After receiving the ACN packet, the source node transmits a Reserve Sectors (RES) packet to reserve the time required to complete the transmission. Nodes that overhear the ACN or the RES packet and are not involved in the current communication, being in the same sectors, defer access and return to the S-IDLE state. After the three-way handshake of ART, ACN, and RES packet exchange, the nodes typically perform full-duplex data transmission. Each data packet is followed by an Acknowledgment (ACK) packet from the respective receiver neighbour node. After the data packet exchange gets completed, both nodes return to the S-IDLE.

VL-MAC has been extended to exploit all the VuLCAN capabilities. For the low-cost VLC hardware systems that do not support full-duplex communication, there is a provision that the receiver node transmits a busy tone signaling. This ensures that other nodes sense the channel to be busy from both directions of the source-destination pair and reduces the hidden node problem. However, in practical

scenarios, to precisely detect from which node the tone is being heard, additional circuitry and algorithms are required.

The VL-MAC protocol assumes to have different channels for control and data packet transmission. This ensures that no collision will occur between data signals and control signals, but it also increases the circuit complexity and energy consumption as well. The protocol adopts the approach of the time-synchronous sector traversal of the nodes to mitigate deafness. In static scenarios, there is a possibility that not every sector of the node has a neighbour corresponding to it. This, in turn, results in empty slots in the VL-MAC protocol's super-slot structure, which can eventually lead to slot wastage and add on to additional latency.

The FOV of the LEDs and PDs are considered to be 45° [38] and mentioned that the solution should be straightforward to extend to any FOVs of LED and PD available in the market. However, the performance evaluation results show a considerable variation in the performance with the varying FOV of LEDs and PDs. With the lower FOVs of LEDs and PDs and a higher number of sectors on the node, there is a possibility of very few or a single neighbour node available to the source node for packet transmission in a specific direction. If that particular neighbour node is busy communicating with some other node or if there is an obstacle blockage between the source node and that specific neighbour node, the data transmission will be challenging.

5.4.3 Neighbour Discovery Evaluation

We evaluated the effectiveness of the periodic and event-based neighbour discovery (ND) approaches through simulation-based experiments. We compare their performance with all the three protocols, the standard IEEE 802.15.7 MAC protocol, the VL-MAC, and the proposed Li-MAC protocol with the same setup and scenarios. Sectors on each node varied from 4 to 15 sectors. We considered two complete sector rounds per node for every neighbour discovery session. The time duration between consecutive rounds is considered to be 1000 ms. We have set the periodic duration

of one hour for the neighbour table discovery and maintenance. For the event-based discovery, we have considered three consecutive packet drops of a node as an event to trigger a neighbour discovery for the individual node.

A node cannot transmit both data and discovery packets simultaneously at the same time. Whenever the individual node is going through the discovery packet transmission (be it in an event or periodic neighbour discovery), it waits for the transmission to get over to start its data transmission. Similarly, if there is ongoing data transmission, the neighbour discovery can only begin once that transmission session is over. Thus, the individual node discovery, which is a one-way transmission of packets, is pretty fast. Moreover, VLC being a directional network provides much better spatial reuse capacity. Thus the in-between neighbour discovery does not result in heavy collisions and affects the network the way it could have been for RF networks.

The following metrics are considered for the evaluation:

- Neighbour Discovery Time, defined as the total time spent by the network in the neighbour discovery of the network.
- Control Packet Overhead, defined as the normalized control packet overhead generated during the network neighbour discovery.

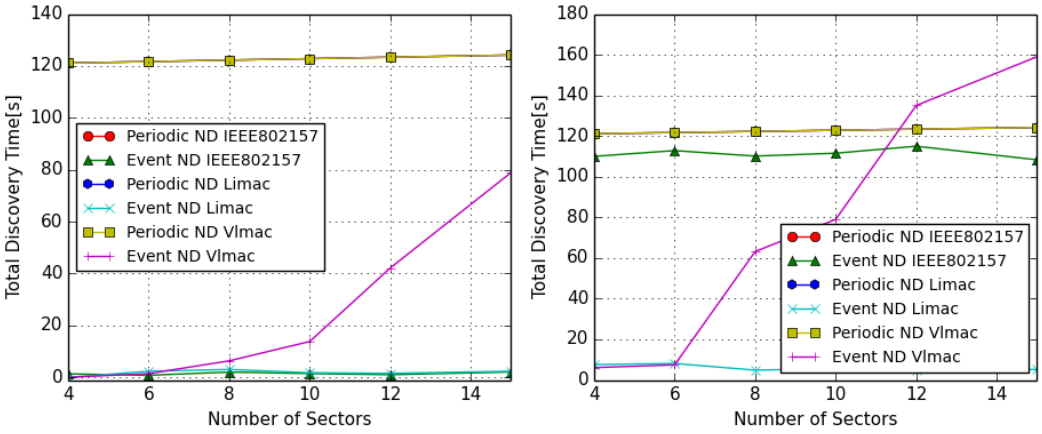

(a) Blocking probability = 20% **(b)** Blocking probability = 40%

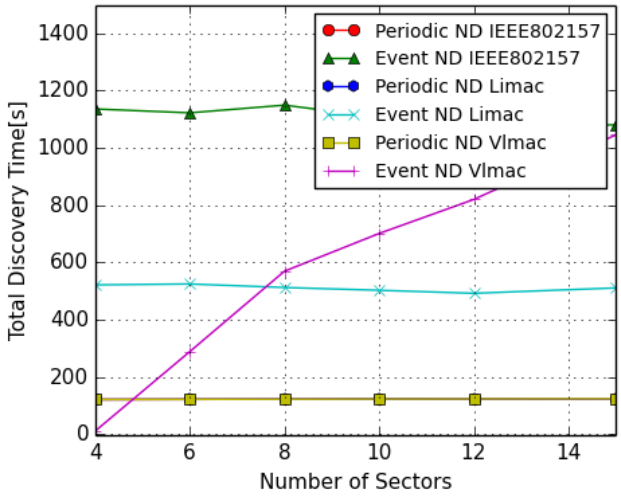

(c) Blocking probability = 60%

Figure 5.8. Comparison of Total Neighbour Discovery Time for Periodic and Event-based Neighbour Discovery(ND) Approaches

- **Neighbour Discovery Time**

  As we can observe from the Figures 5.8, the time taken by periodic neighbour discovery time is almost the same for all the three protocols with varying blocking probability with slight variation with the increase in sectors. It takes around 120 seconds for the complete network discovery in a periodic serialized approach. Whereas for the event-based neighbour discovery, it varies based on the protocol and the blocking probability. For the IEEE 802.15.7

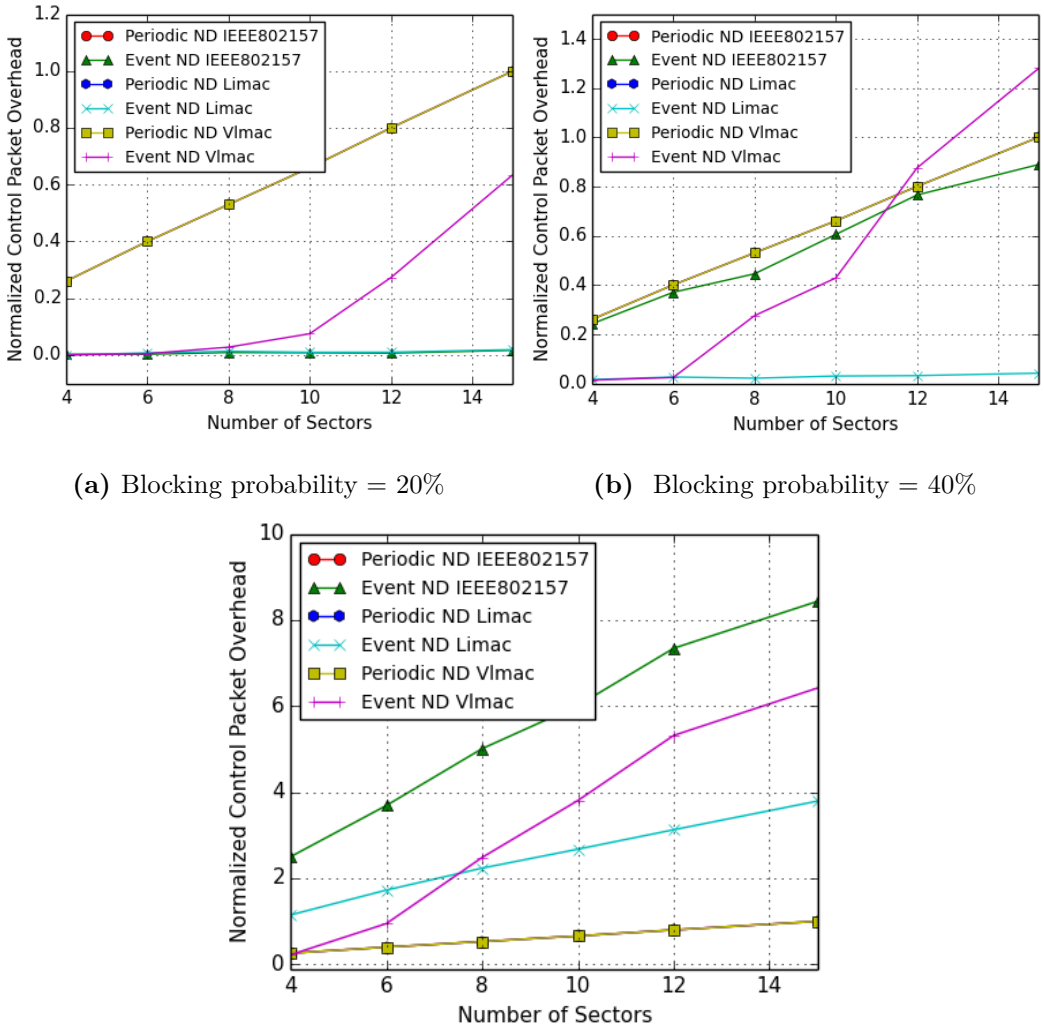

(a) Blocking probability = 20%

(b) Blocking probability = 40%

(c) Blocking probability = 60%

Figure 5.9. Control packet overhead: Periodic vs. event-based neighbour discovery

protocol, the event-based neighbour discovery time is under 5 seconds for 20% blocking probability, but it increases with higher blockages. With higher blocking probability, the packet drops are more frequent in the IEEE 802.15.7 protocol than the other two protocols, resulting in more frequent triggering of the neighbour discovery. Thus the neighbour discovery time reaches around 1100 seconds. The Li-MAC protocol is equipped to handle directionality and deafness, which lowers the need for neighbour discovery frequently. Thus event-based approach could save energy and time for the network. In the VL-MAC

protocol, the event-based ND frequency increases drastically with the higher number of sectors and with blocking probability and becomes more than 1000 seconds. Thus, in general, event-based triggering is a better approach at lower blocking probability than periodic neighbour discovery. Whereas with increasing blocking probability, the neighbour discovery approach should be selected based on the protocol and the sectors involved.

- **Control Packet Overhead** Figure 5.9 shows the normalized control packet overhead for periodic and event-based neighbour discovery for the increasing number of sectors and varying blocking probability for all three protocols. In periodic neighbour discovery, the control overhead values are almost identical for all three protocols. For 20% blocking probability, the control overhead is around 1.57 times lower in event-based than periodic for all the three protocols. However, with the increase in blocking probability, the triggering due to packet drop increases and thus increases the control packet overhead, making it eight times more than the periodic discovery overhead in the IEEE 802.15.7 MAC protocol. With the increase in sectors, the triggering increases in VL-MAC protocol, resulting in 6.47 times higher control packet overhead with 15 sectors per node compared to 4 sectors per node.

5.4.4 Simulation Scenario

We consider a connected VLC network made up of 60 nodes in an indoor static scenario. Each node in the network is capable of sensing and communicating with all its neighbouring nodes. Moreover, nodes are randomly and uniformly distributed over a square area of size 14×14 m^2. The sector value was selected to be within the range of FOVs of LED and PD available in the market. The blocking probability is varied in the range of 20% to 60% to simulate realistic blockage scenarios. The data generation occurs according to a Poisson process of intensity λ packets per second. In our simulation results, we make use of the inter-arrival time between packets, which is defined as packetSpacing = $1/\lambda$ and ranges from 50 to 5000 milliseconds

(ms). Once a packet is generated, a source node is randomly chosen among all the available nodes. Each data packet has a size of 65B, including payload and headers added by lower layers. The size of the control packets is 19B. The channel data rate is set to 65Kbps. A periodic neighbour discovery scheme is adopted for all three protocols to ensure a fair comparison. All three MAC protocols are evaluated under the standard directional routing scheme. Each packet transmission in the network involves a source node and the fixed sink in the network. The sink is located at the bottom left of the topology at the origin (0,0). All the nodes in the network are aware of the sink location. The sink is used to determine the direction of the forward progress for the source nodes. Based on the individual MAC protocol, the node chooses the next suitable neighbour node and the way it attempts to forward the packet to the neighbour node. If no neighbour node is available to forward the packet in the direction towards the sink for that individual node, the packet is sent to any available neighbour node at that time. The maximum number of hops is limited to five hops; If the packet has not reached the sink destination in that many hops, the respective packet will be dropped.

The simulation parameters are summarized in table 5.1.

5.4.5 Investigated Metrics

The following metrics are considered for the evaluation of the MAC protocol proposed:

- Packet Delivery Ratio (PDR), defined as the ratio of data packets successfully delivered to the original generated data packets.
- The Average Energy Consumption per node, defined as the average amount of energy spent by an individual node to transmit and receive the packets and sense and listen to the channel during the simulation.
- The Energy Efficiency, defined as the total energy consumption of the network to the number of successfully delivered packets to the sink.

Table 5.1. Simulation Parameters

Definition	Value
Simulation duration(Ts)	6 hours
Deployment area size	14 × 14m2
Number of nodes	60
Sectors of LEDs and PDs	[4,15]sectors
Channel data rate	65Kbps
Packet Spacing	[50,5000] ms
Blocking Probability	[20,40,60]%
VLC range	5m
K	3
N	3

- End-to-End Per Packet Latency, defined as the time from packet generation to its correct delivery to the sink.

All results have been obtained by averaging the outcomes of 38 simulation runs, each of duration Ts of 6 hours.

5.4.6 Simulation Results

- **Packet Delivery Ratio**

  Li-MAC clearly outperforms the other two strategies in PDR performance in terms of a varying number of sectors, the blocking probability, and also with an increase in traffic as shown in Figures 5.10, 5.11 and 5.12. At 20% and 40% blocking probability (low and medium blockage scenarios), Li-MAC delivers more than 90% of the packets for a lower number of sectors (higher FOV of LED and PD) regardless of the traffic load as shown in Figures 5.10c and 5.11c.

The performance improvement depends on the directional handshaking and virtual carrier sensing mechanisms enacted by Li-MAC, which help deal with hidden terminal and directionality issues. The busy node beaconing technique reduces deafness in the directional VLC network.

While in VL-MAC, as observed from Figures 5.10b and 5.11b., the PDR is close to 90% for lower/medium traffic and lower number of sectors but sharply decreases with higher traffic. A time-synchronous utility-based opportunistic three-way handshake and busy tone signaling are employed to deal with VLC challenges in VL-MAC protocol. However, this strategy has a control packet overhead, which is approximately 2.85 times higher than Li-MAC, as shown in Figures 5.13, 5.14 and 5.15. Different channels for control and data packet and busy tone signaling increase the circuit complexity and energy consumption. The PDR attained by IEEE 802.15.7 CSMA/CA protocol is around 85% and 61% for the 20% and 40% blocking probability, respectively, which is lower than the other two protocols discussed, as shown in Figures 5.10a and 5.11a; The main reason being the hidden node and directionality issues with the simple IEEE 802.15.7 CSMA/CA scheme. Also, there is no mechanism to deal with deafness which results in re-transmissions up to 65% of data packets and leads to packet loss, as shown in Figures 5.16a, 5.17a and 5.18a.

At the extreme high obstacle blockage scenario (60% blocking probability), the average PDR is around 30% for the IEEE 802.15.7 MAC protocol, as shown in Figure 5.12a. The protocol targets one destination node, which provides a source node with only one possible relay. If there is a consistent blockage, the packet will be discarded by the sender after a predetermined number of transmission attempts, thus suffers from heavy packet loss. The PDR performance for Li-MAC and VL-MAC in high blockage conditions with a lower number of sectors is 76% and 72%, respectively.

However, the PDR for VL-MAC decreases more sharply with an increase in the number of sectors and drops to 20% with increased traffic as observed from Figure 5.12b. as compared to Li-MAC protocol which drops to 30% for the highest traffic load for the lower sectors. VL-MAC is a time-synchronous and slot-based protocol, and so if there are consistent blockages between the ongoing transmission, it can get more challenging to resume and maintain the ongoing communication and result in packet loss. Due to the same reason, VL-MAC cannot cope up with the highest traffic, and its PDR drop to 6% because the latency for VL-MAC protocol is very high for end-to-end transmission, which is around four times that incurred by Li-MAC as further discussed in detail in the following points. Li-MAC provides a better strategy to deal with blocking; If there is no response from the targeted neighbour node, the source node attempts to send the packet through another neighbour node, be it in the same or different sector, which increases the chance of finding a relay node. Therefore, the PDR for Li-MAC is comparatively higher than the other two protocols.

For lower FOV of LEDs and PDs (higher number of sectors) on the node, which is a highly directional scenario, finding a neighbour node in the required specific direction can be challenging. The Li-MAC protocol PDR performance is up to 1.5 and 3.5 times better than IEEE 802.15.7 CSMA/CA and VL-MAC protocol, respectively, due to the Li-MAC characteristics described above. Li-MAC, also being an asynchronous and comparatively light protocol, can support very small packet inter-arrival time and thus work even better at high traffic scenarios. However, the PDR for VL-MAC drops to 6% for lower FOV of LEDs and PDs (higher number of sectors) as shown in Figure 5.12b since VL-MAC selects a specific sector based on the utility function and broadcasts an ART request through that sector. If the FOV is large (lower number of sectors on the node, hence broader coverage), there is a high possibility of receiving an ACN (availability confirmation) from the neighbour node. However, for lower FOVs scenario (higher number of sectors), there might be very few nodes that receive the ART request. If they are already busy or blocked by an

obstacle, it results in a reduction of PDR. With the higher number of sectors (lower FOV of LEDs and PDs) on the node and, in turn, in highly directional nodes, there is a possibility of increased hops in the network. Therefore, if there is a limitation on the number of hops or on the packet arrival time at the final destination, it will lead to packet drops.

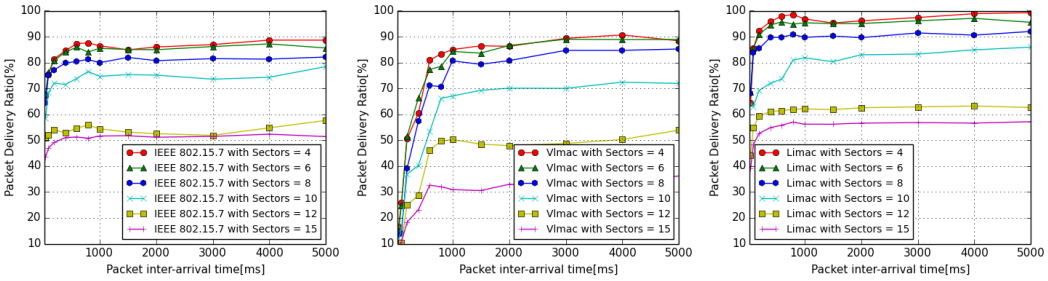

(a) IEEE 802.15.7 CSMA/CA MAC Protocol **(b)** VL-MAC MAC Protocol **(c)** Li-MAC MAC Protocol

Figure 5.10. Comparison of Packet Delivery Ratio (PDR) with Blocking probability = 20%

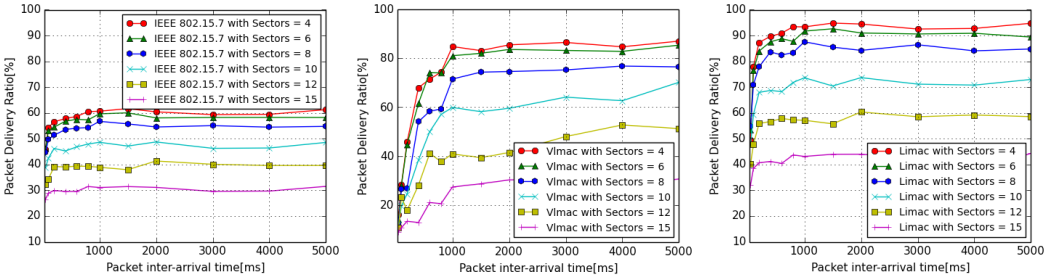

(a) IEEE 802.15.7 CSMA/CA MAC Protocol **(b)** VL-MAC MAC Protocol **(c)** Li-MAC MAC Protocol

Figure 5.11. Comparison of Packet Delivery Ratio (PDR) with Blocking probability = 40%

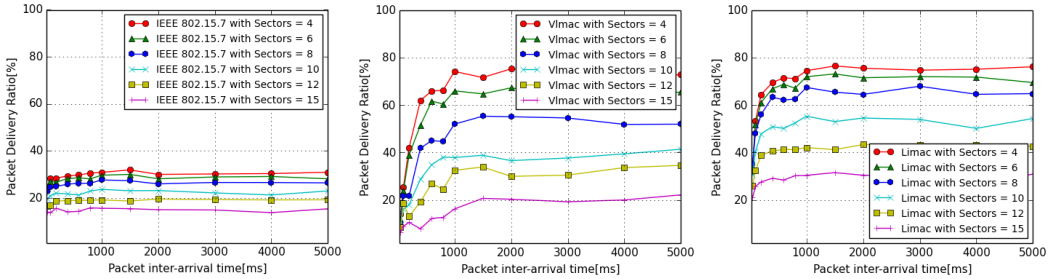

(a) IEEE 802.15.7 CSMA/CA **(b)** VL-MAC MAC Protocol **(c)** Li-MAC MAC Protocol MAC Protocol

Figure 5.12. Comparison of Packet Delivery Ratio (PDR) with Blocking probability = 60%

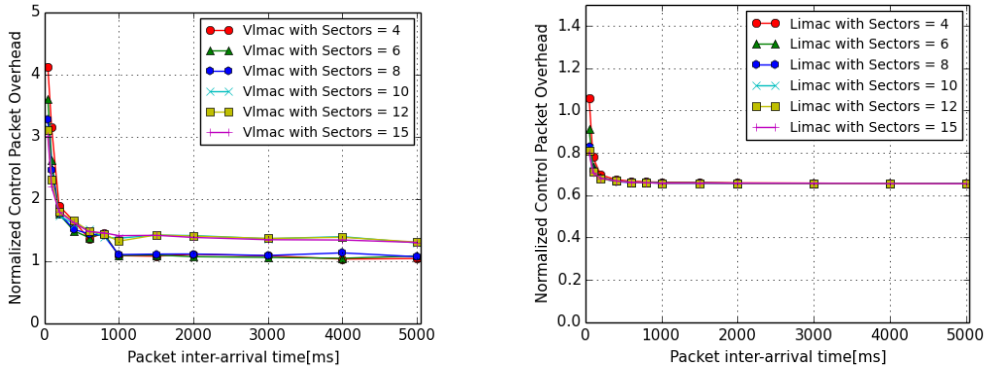

(a) VL-MAC MAC Protocol **(b)** Li-MAC MAC Protocol

Figure 5.13. Comparison of Control Packet Overhead with Blocking probability = 20%

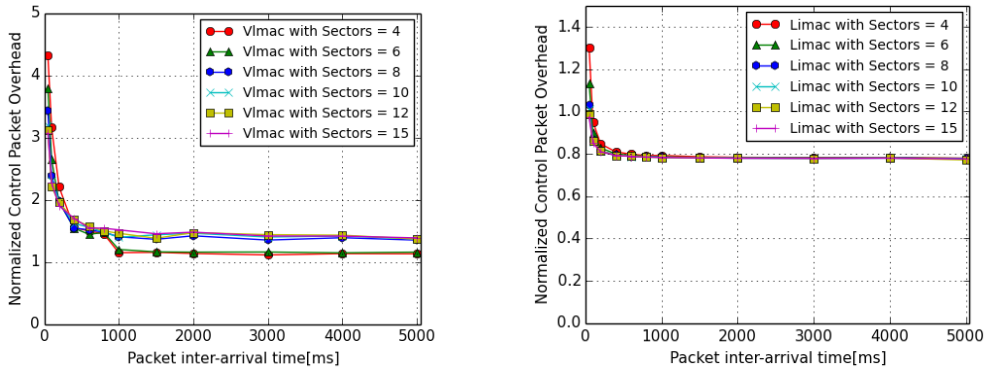

(a) VL-MAC MAC Protocol **(b)** Li-MAC MAC Protocol

Figure 5.14. Comparison of Control Packet Overhead with Blocking probability = 40%

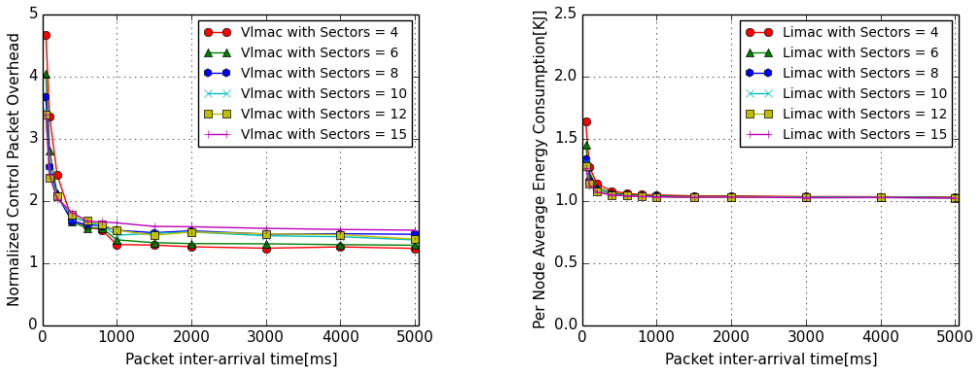

(a) VL-MAC MAC Protocol **(b)** Li-MAC MAC Protocol

Figure 5.15. Comparison of Control Packet Overhead with Blocking probability = 60%

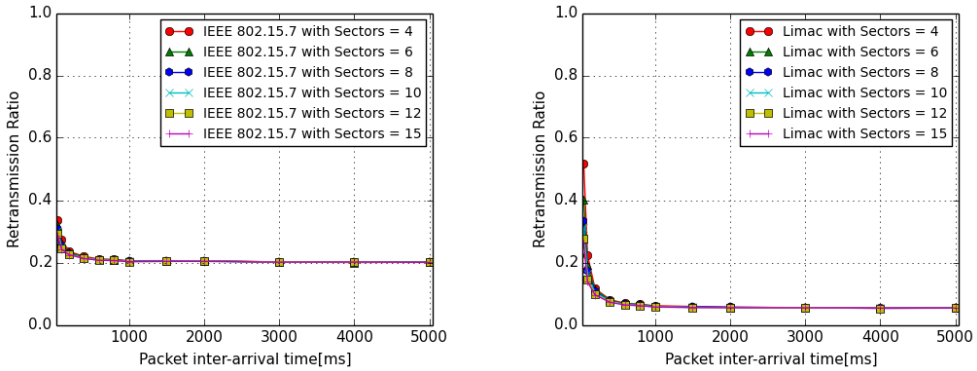

(a) IEEE 802.15.7 CSMA/CA MAC Protocol **(b)** Li-MAC MAC Protocol

Figure 5.16. Comparison of Retransmission ratio with Blocking Probability = 20%

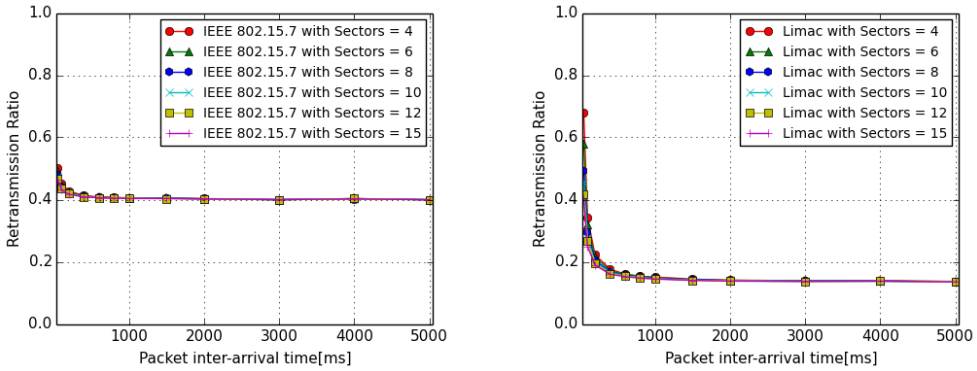

(a) IEEE 802.15.7 CSMA/CA MAC Protocol **(b)** Li-MAC MAC Protocol

Figure 5.17. Comparison of Retransmission ratio with Blocking Probability = 40%

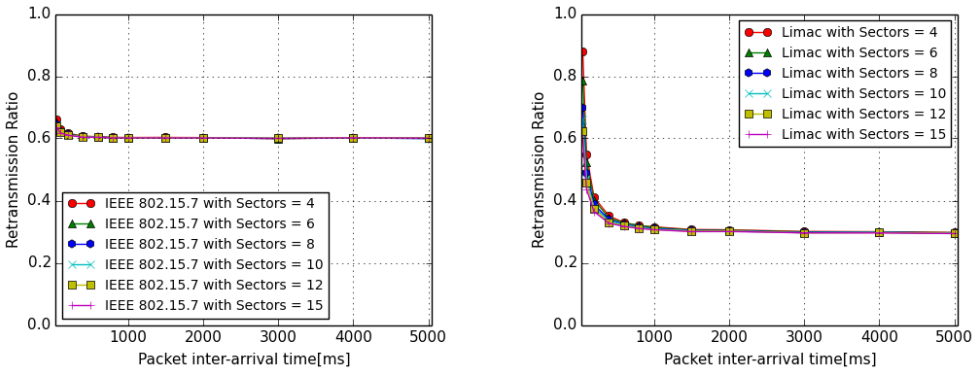

(a) IEEE 802.15.7 CSMA/CA MAC Protocol **(b)** Li-MAC MAC Protocol

Figure 5.18. Comparison of Retransmission ratio with Blocking Probability = 60%

- **Per Node Average Energy Consumption**

  Figures 5.19, 5.20 and 5.21 show the per node average energy consumption of all the three protocols. The IEEE 802.15.7 MAC protocol, being the simplest protocol, with no additional control packets overhead, has the lowest energy consumption, which is below 1.46 KJ among all the three protocols, as shown in Figures 5.19a, 5.20a and 5.21a. It is up to 1.5 and 2.5 times less energy-consuming per node as compared to Li-MAC and VL-MAC protocols, respectively. However, it suffers from the highest packet loss. Although there are no control packet exchanges in the IEEE 802.15.7 MAC protocol, the energy consumption is mainly due to the higher data packets re-transmission, which is up to 65 % along with the standard transmissions at the highest blockage and the highest traffic scenario as shown in Figures 5.19, 5.20 and 5.21.

  Figures 5.19b, 5.20b and 5.21b show the average energy consumption per node for the VL-MAC protocol. The highest energy consumption is around 3.60 KJ. The energy per node consumption of the VL-MAC protocol is highest as compared to the other two protocols due to higher control packet exchanges as it is a time-synchronized protocol along with the broadcasting of ART packets which results in additional overhead. With higher FOV of individual LED and PD on the node (lower number of sectors), the nodes under coverage increase,

and more neighbour nodes can receive the broadcast ART packet. In turn, more number of ACN packets are transmitted to the source node, resulting in higher control packet exchanges, higher chances of interferences, and thus higher consumption of energy.

The average energy consumption per node for Li-MAC protocol is shown in Figures 5.19c, 5.20c and 5.21c, spending up to 1.68 times less energy than VL-MAC protocol despite its higher PDR. There is an increase in energy consumption at the highest traffic and reaches up to 2.2 KJ, but there is not much variation with the higher number of sectors on the node.

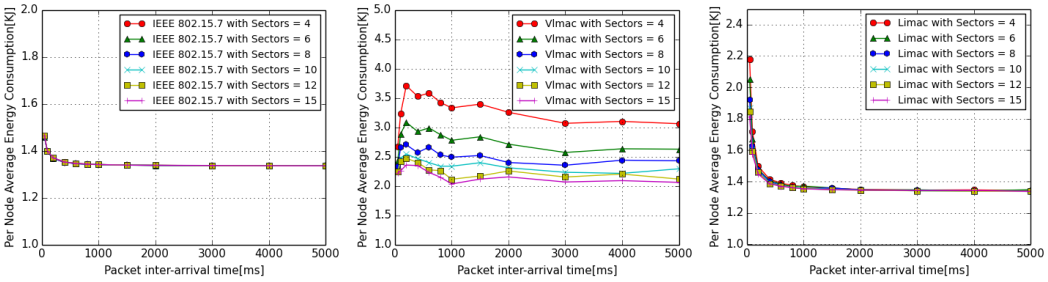

(a) IEEE 802.15.7 CSMA/CA MAC Protocol **(b)** VL-MAC MAC Protocol **(c)** Li-MAC MAC Protocol

Figure 5.19. Comparison of Per Node Average Energy Consumption with Blocking probability = 20%

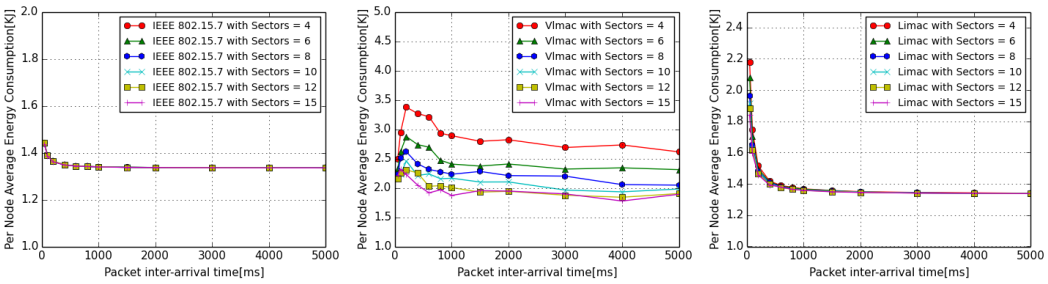

(a) IEEE 802.15.7 CSMA/CA MAC Protocol **(b)** VL-MAC MAC Protocol **(c)** Li-MAC MAC Protocol

Figure 5.20. Comparison of Per Node Average Energy Consumption with Blocking probability = 40%

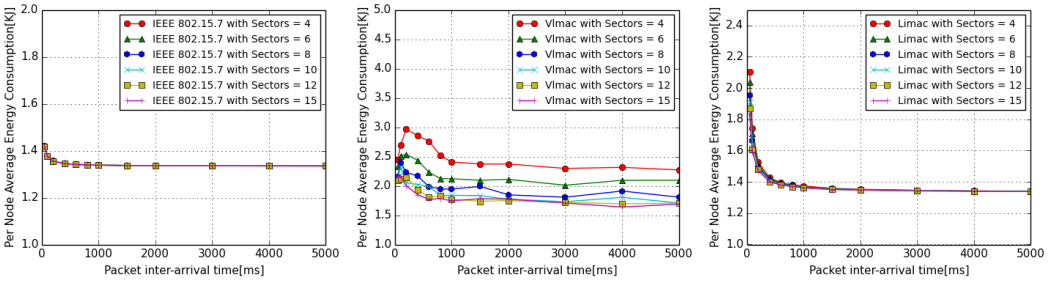

(a) IEEE 802.15.7 CSMA/CA **(b)** VL-MAC MAC Protocol **(c)** Li-MAC MAC Protocol
MAC Protocol

Figure 5.21. Comparison of Per Node Average Energy Consumption with Blocking probability = 60%

Figures 5.22 and 5.23 depict results that allow us to delve deeper into the differences of the three strategies concerning their use of energy. It show the energy efficiency of the network, which is defined as,

$$\text{Energy Efficiency} = {}^{1}/\left(\frac{\text{Number of Successfully Delivered Packets to the Sink}}{\text{Total Energy Consumption of the Network}}\right) \tag{5.3}$$

These energy efficiency values reflect the energy utilization of the three strategies. The smaller the value of the slope and the smaller the curve fluctuation, the more balanced the energy utilization of the network. The more balanced the energy utilization, the greater the network's energy efficiency and the longer the network lifetime. We have considered a specific scenario representative of typical performance. This scenario refers to a network of 60 nodes with FOV of LED and PD to be 45°(sector = 4) and 12°(sectors = 15) respectively, with blocking probability scenarios ranging from 20% to 60%. It is clear that Li-MAC is the most efficient among all three strategies. For example, in the case of 45°FOV (sectors = 4) and for the lower blocking scenarios, Li-MAC is 1.15 and 2.95 times more energy-efficient than IEEE 802.15.7 CSMA/CA and VL-MAC, respectively. Whereas for heavy blockage scenarios of 60% blockage probability, Li-MAC is 2.42 and 1.96 times more efficient as compared to the IEEE 802.15.7 CSMA/CA protocol and VL-MAC, respectively.

For the case of 12°(sectors = 15), which is a lower FOV (higher number of sectors) scenario, as can be observed from the Figures 5.22 and 5.23, the overall

energy efficiency is lower than that for higher FOVs (lower sectors) of LED and PD on the nodes. However, Li-MAC performance is comparatively better than the other two strategies. For higher blocking probability, Li-MAC is 2 and 2.16 times more efficient as compared to the IEEE 802.15.7 CSMA/CA and VL-MAC protocol, respectively. These plots also help in better understanding of the hardware design choices which could be made regarding the FOVs of LEDs and PDS on the nodes for the VLC networks.

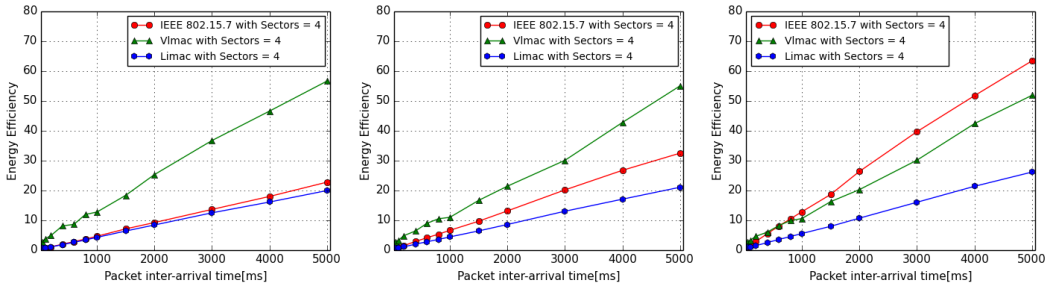

(a) Energy Efficiency with Blocking Probability = 20%

(b) Energy Efficiency with Blocking Probability = 40%

(c) Energy Efficiency with Blocking Probability = 60%

Figure 5.22. Comparison of Energy Efficiency with sectors = 4 for the three strategies

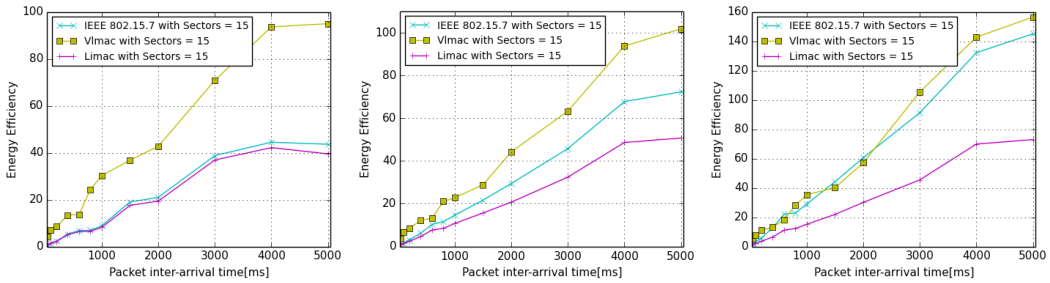

(a) Energy Efficiency with Blocking Probability = 20%

(b) Energy Efficiency with Blocking Probability = 40%

(c) Energy Efficiency with Blocking Probability = 60%

Figure 5.23. Comparison of Energy Efficiency with sectors = 15 for the three strategies

The effectiveness of our approach is further demonstrated by providing a quantitative assessment of the per-node energy consumption of a sample topology. Figure 5.24 shows the snapshot of a selected, exemplary topology. It shows a network of 59 nodes plus the sink, with the sink placed at the bottom left corner (depicted as a black triangle). Network nodes are depicted as circles. This scenario refers to a network with medium/high traffic (the packet inter-arrival time is 1s). In our results, the FOV of the LED and PD considered is 45°with a 20% blocking probability. The color of a node indicates the energy it consumed throughout the simulation time. The colour strip is represented by rainbow VIBGYOR. The more towards red the color, the higher the energy consumed, and the more towards violet the colour, the lower the energy consumed. The range of the bar at the right of Figures 5.24a, 5.24b and 5.24c are kept same to ensure fair comparison of the per node energy consumption.

We observe that VL-MAC nodes are colored more towards green and yellow shades, indicating higher overhead and control packet exchanges, thus energy consumption per node compared to IEEE 802.15.7 and Li-MAC protocols. VL-MAC broadcast ART packets to all the nodes falling in the sector chosen for communication. Also, the optimized sector is normally the one with more number of reachable neighbouring nodes. As a result, the nodes placed at the center of the square receive more packets than those toward the perimeter of the deployment area and, in turn, have more energy consumption, as depicted by the colours in the Figure 5.24b.

A more detailed zoomed snapshot of the energy distribution per node for IEEE 802.15.7 and Li-MAC is shown in Figure 5.25. As there are no control packet exchanges, the consumption of energy by IEEE 802.15.7 is the lowest among all three protocols. The nodes in the Li-MAC protocol are mainly colored in violet and blue, showing a proper balance and higher energy efficiency throughout the network. The more sparsely located nodes tend to consume more energy as they would act as relays for more transmissions in Li-MAC and IEEE 802.15.7.

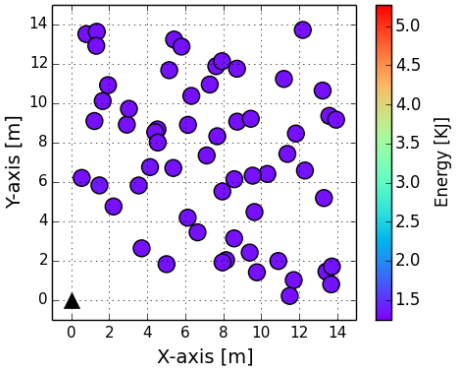

(a) IEEE 802.15.7 CSMA/CA: Energy consumption

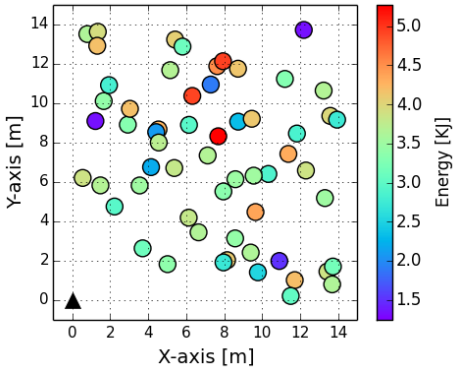

(b) VL-MAC: Energy consumption

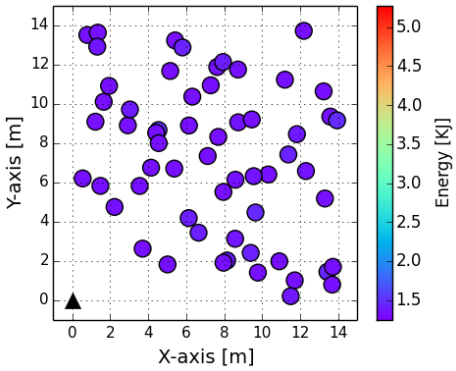

(c) Li-MAC: Energy consumption

Figure 5.24. Per node energy consumption in networks with inter-arrival time of 1 second

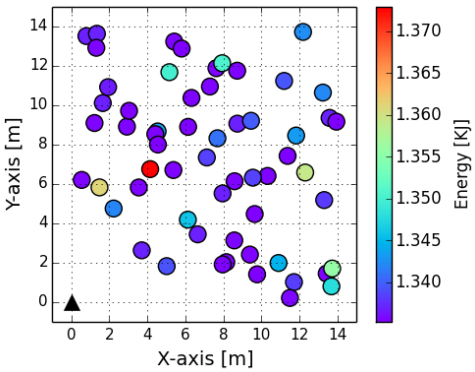

(a) IEEE 802.15.7 CSMA/CA: Energy consumption

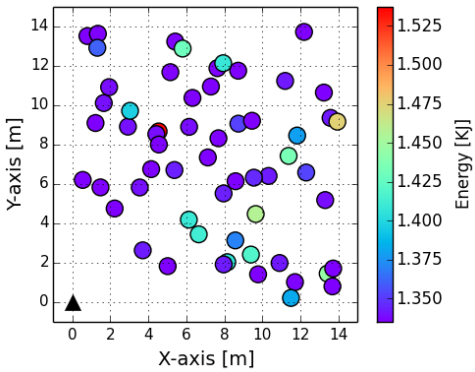

(b) Li-MAC: Energy consumption

Figure 5.25. Zoomed-in Distribution of Per node energy consumption in networks with inter-arrival time of 1 second

- **End-to-End Per Packet Latency** The average packet end-to-end latency for the three protocols is shown in Figures 5.26, 5.27, and 5.28 for the blocking probabilities ranging from 20% to 60%. In all the three scenarios of blocking probability, the IEEE 802.15.7 CSMA/CA attains the lowest average latency, as shown in Figures 5.26a, 5.27a and 5.28a compared to the other two protocols. It achieves a per-packet latency up to 3 and 10 times lower than that incurred by Li-MAC and VL-MAC, respectively. The reason being the relatively simple protocol without any control packet exchanges, but it incurred the highest PDR loss.

  Figures 5.26c, 5.27c and 5.28c show the average latency of the Li-MAC protocol. Although Li-MAC delivers significantly more packets irrespective of traffic and number of sectors, it achieves a per-packet latency, which is up to 4 times lower than that incurred by VL-MAC. Li-MAC is an asynchronous protocol and does not follow slot-based synchronization in the network. Instead, it listens with all its low-power PDs ON in the listening mode, which saves a lot of time and lowers the per-packet latency. Also, the control packet exchanges in Li-MAC are 2.85 times less than the VL-MAC protocol, as shown in Figures 5.13, 5.14 and 5.15.

  Figures 5.26b, 5.27b and 5.28b show the average latency of the VL-MAC protocol. The average latency is in the range of 450 to 580 ms, which is relatively high compared to the other two protocols. This is mainly due to the following reasons. First, VL-MAC follows a strict time slot allotment per sector and synchronization among the nodes. Secondly, the super-frame structure has a dedicated slot for each sector, and thus, the higher number of sectors, the more time it takes in traversing through all the sector slots.

  As observed from the Figures 5.26, 5.27, and 5.28, there is a slight increase in latency for all three protocols with the increase in blocking probability, as more blockage obstacles result in more control packets and data packets re-transmissions.

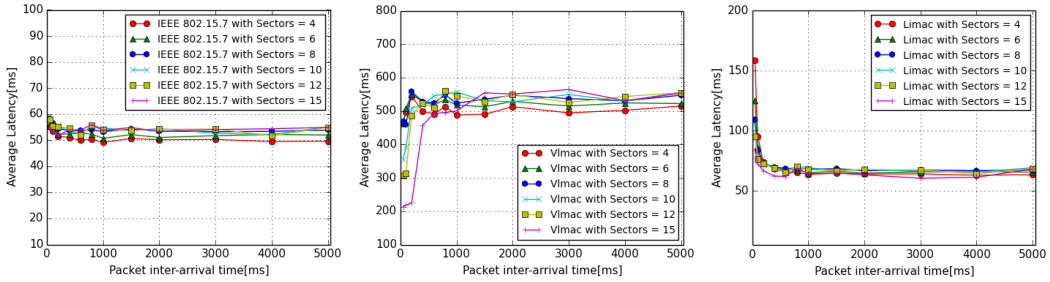

(a) IEEE 802.15.7 CSMA/CA **(b)** VL-MAC MAC Protocol **(c)** Li-MAC MAC Protocol MAC Protocol

Figure 5.26. Comparison of Average Latency with Blocking probability = 20%

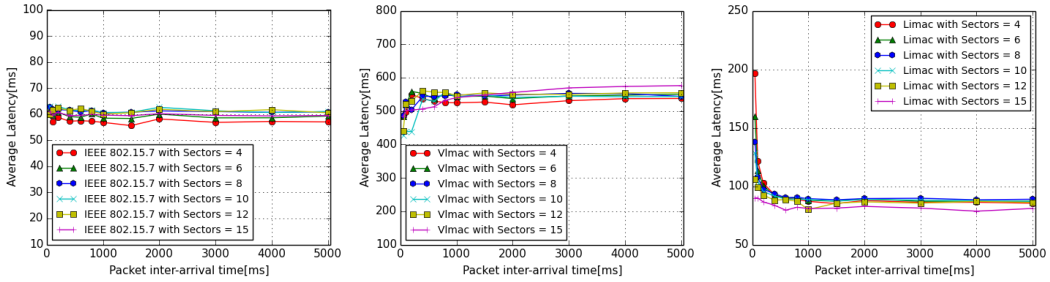

(a) IEEE 802.15.7 CSMA/CA **(b)** VL-MAC MAC Protocol **(c)** Li-MAC MAC Protocol MAC Protocol

Figure 5.27. Comparison of Average Latency with Blocking probability = 40%

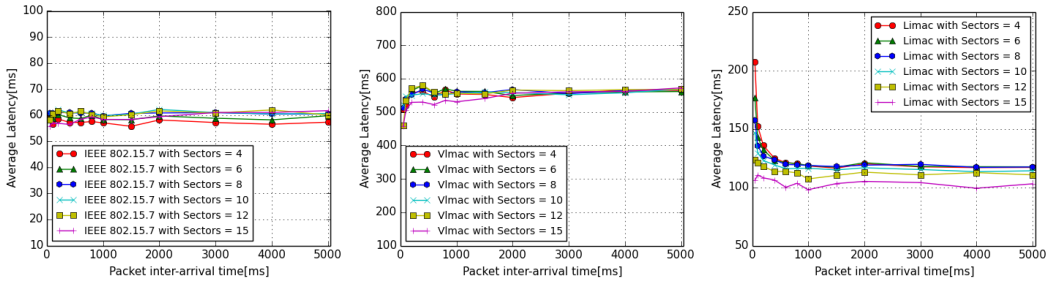

(a) IEEE 802.15.7 CSMA/CA **(b)** VL-MAC MAC Protocol **(c)** Li-MAC MAC Protocol MAC Protocol

Figure 5.28. Comparison of Average Latency with Blocking probability = 60%

5.5 Summary

- Li-MAC clearly outperforms the other two strategies in PDR performance across considered scenarios when varying number of sectors, the blocking probability, and also with an increase in traffic as shown in Figures 5.10, 5.11 and 5.12. as Li-MAC delivers more than 90% of the packets for a lower number of sectors (higher FOV of LED and PD) regardless of the traffic load.
- While in VL-MAC, as observed from Figures 5.10b and 5.11b., the PDR is close to 90% for lower/medium traffic and lower number of sectors but sharply decreases with higher traffic.
- Also, VL-MAC has a control packet overhead, which is approximately 2.85 times higher than Li-MAC, as shown in Figures 5.13, 5.14 and 5.15.
- The PDR attained by IEEE 802.15.7 CSMA/CA protocol is around 85% and 61% for the 20% and 40% blocking probability, respectively, which is lower than the other two protocols discussed, as shown in Figures 5.10a and 5.11a.
- There is no mechanism to deal with directionality and deafness in IEEE 802.15.7 CSMA/CA which results in re-transmissions upto 65% of data packets and leads to packet loss, as shown in Figures 5.16a, 5.17a and 5.18a.
- For lower FOV of LEDs and PDs (higher number of sectors) on the node, which is a highly directional scenario, Li-MAC protocol PDR performance is up to 1.5 and 3.5 times better than IEEE 802.15.7 CSMA/CA and VL-MAC protocol, respectively. Li-MAC, also an asynchronous and comparatively light protocol, can support very small packet inter-arrival time and thus work even better at high traffic scenarios.
- At the extreme high obstacle blockage scenario (60% blocking probability), the average PDR is around 30% for the IEEE 802.15.7 MAC protocol, as shown in Figure 5.12a. The PDR performance for Li-MAC and VL-MAC in high blockage conditions with a lower number of sectors is 76% and 72%, respectively. However, the PDR for VL-MAC decreases more sharply with an

increase in the number of sectors and drops to 20% with increased traffic as observed from Figure 5.12b as compare to Li-MAC protocol which drops to 30% for the highest traffic load for the lower sectors.

- The average packet end-to-end latency for the three protocols as shown in Figures 5.26, 5.27, and 5.28. is in the range of 60 ms, 100 ms, and 500 ms for IEEE CSMA/CA, Li-MAC, and VL-MAC protocols, respectively; VL-MAC follows a strict time slot allotment per sector and synchronization among the nodes, which results in high end to end latency.

- IEEE CSMA/CA is a relatively simple protocol without any control packet exchanges, but it incurred the highest PDR loss. Although Li-MAC delivers significantly more packets in comparison to VL-MAC and IEEE CSMA/CA strategies irrespective of traffic and number of sectors, it achieves a per-packet latency, which is up to 4 times lower than that incurred by VL-MAC as Li-MAC is an asynchronous protocol and does not follow slot-based synchronization in the network.

- Figures 5.19, 5.20 and 5.21 show the per node average energy consumption of all the three protocols. The IEEE 802.15.7 MAC protocol, being the simplest protocol, has the lowest energy consumption, which is below 1.46 KJ among all the three protocols, but it suffers heavy packet losses. VL-MAC has the highest energy consumption, which is around 3.60 KJ. Li-MAC has an average energy consumption per node up to 2.2 KJ at the increased traffic, spending up to 1.68 times less energy than the VL-MAC protocol despite its higher PDR.

- Figures 5.22 and 5.23 show the energy efficiency of the network. The smaller the value of the slope and the smaller the curve fluctuation, the more balanced the energy utilization of the network; It is clear from the graphs that Li-MAC is the most efficient among all three strategies.

5.6 Conclusions

In this work, we have presented Li-MAC, an asynchronous MAC layer protocol for low cost and low power ad-hoc VLC networks. Li-MAC, being an asynchronous protocol, utilizes a directional handshaking mechanism, virtual carrier sensing, and busy node beaconing to alleviate hidden node terminal, deafness, and blockage issues. We compared the performance of Li-MAC with the standard IEEE 802.15.7 CSMA/CA and VL-MAC, two state-of-art MAC protocols for VLC networks through Green Castalia simulations with varying traffic, blocking conditions, and FOVs of LED and PD on the node. Results show that the proposed Li-MAC protocol outperforms the other two strategies in PDR performance and energy efficiency irrespective of the traffic load, blocking conditions, and FOVs of LED and PD while consuming considerably less energy and delivering packets faster.

CHAPTER 6

Concluding Remarks

With the rise of the Internet of Things, billions of devices are wirelessly interacting with each other. Though RF solutions exist, they are sometimes not the most suitable for indoor and outdoor scenarios due to the spectrum's overcrowding, power consumption, and radiations. While looking for an alternative wireless solution raises the following question: since these days, almost all the indoor settings already integrates LED lighting, which is energy and cost-effective and with a fast switching rate, can we leverage them for communication using VLC ? That is this question that has become the main drive of this thesis. This thesis aims at starting the exploration of the use of VLC to enable low-cost and low-power VLC networking among IoT devices. It also attempts to provide insights about which design choices are best for achieving the performance needed by low-cost and low-power ad-hoc VLC networks.

To reach this targetted goal, we have attempted to solve many issues that improve the baseline state of the art. Chapter 2 summarizes state-of-the-art on low-end, embedded VLC prototypes. This study highlights the lack of contributions and an optimized solution to provide a balance between data rate, range, power, and reliability in varied ambient noise conditions. The second part of Chapter 2 focuses on the limited works on a dedicated VLC network simulator. The last section aims

to provide a brief review of the current state-of-the-art MAC protocols for VLC networks. Studies on protocol design, performance comparisons based on proper simulators considering the physical layer, and solution testing for VLC ad-hoc networking are still uncharted territory.

We begin our work by proposing a software-defined VLC prototype named VuLCAN for Visible Light Communication And Networking in Chapter 3. VuLCAN is an ambient noise-resistant, low-cost, low-power, and low-end VLC board that overcomes existing low-end VLC systems' limitations. VuLCAN takes advantage of frequency-based modulation paired with DSP techniques to obtain ambient noise cancellation while maintaining a reasonable communication range, data rate, and low power consumption. Mainly, VuLCAN employs FSK modulation and adopts the Chirp and Goertzel algorithm for signal detection and demodulation, respectively, thus following a software-defined approach. VuLCAN is based on an ARM Cortex M7 core microcontroller with a fast sampling analog-to-digital converter and power-optimized Digital Signal Processing (DSP)libraries. Using BFSK modulation, the prototype achieves a data rate of 65 Kbps over a communication range of 4.5 m. comparable to the state-of-the-art prototypes. VuLCAN also provides robust and reliable communications in highly illuminated environments (up to 800 lux) using only a low-power Light Emitting Diode (LED), largely exceeding the capabilities of current state-of-the-art prototypes.

Based on the insights and experiences gained while testing VuLCAN and relying on the classic Lambertian radiator model, we extended the capabilities of the open-source GreenCastalia simulator to model wireless channel and RADIO layers for VLC as presented in Chapter 4. GreenCastalia is an extension of the widely used Castalia simulator used to model energy-related aspects of wireless sensor networks accurately. Simulations play an important role in the development by being a cost and time-effective tool to test the algorithms and protocols. This implementation of the wireless channel and RADIO layer for the VLC can be utilized to study upper-layer protocols for VLC, as demonstrated in Chapter 5. We have also attempted to make the implementation flexible to be used with any VLC prototype and circuitry, which allows us to speed up the design process for the network stack in a wide range

of scenarios.

In Chapter 5, We design and implement a distributed asynchronous MAC protocol named Li-MAC (Light-MAC) protocol along with neighbour discovery schemes explicitly designed to deal with the directional VLC challenges. The design of multiple LEDs and PDs are adopted on the node to provide 360 °angle coverage and omni-directional communication to support ad-hoc VLC networking. Li-MAC protocol is based on a handshaking mechanism and virtual carrier sensing to keep the nodes aware of ongoing communication and, in turn, avoid collisions and interferences without adopting any TDMA or FDMA-based sophisticated techniques. The proposed Li-MAC protocol is implemented and evaluated on Green Castalia with the VLC channel and RADIO as the PHY layer. We also studied the impact of the different field of view (FOV) of the LEDs and PDs on the VLC channel, node connectivity, and protocols. We compared the performance of the proposed MAC protocol, Li-MAC, with that of the state-of-the-art IEEE standard 802.15.7 MAC protocol and multi-utility opportunistic VL-MAC protocol, through extensive simulations. Results show that the proposed strategy outperforms the other two MAC protocols concerning all the considered performance metrics required for low-end ad-hoc VLC networking.

In summary, this thesis focuses on the use of VLC as an alternative technology for IoT networks. We have attempted to solve issues regarding VLC prototypes and network protocols through this thesis, which push the baseline state-of-the-art.

Bibliography

[1] Ieee standard for local and metropolitan area networks–part 15.7: Short-range wireless optical communication using visible light. *IEEE Std 802.15.7-2011* (2011), 1–309.

[2] Ieee standard for information technology—telecommunications and information exchange between systems local and metropolitan area networks—specific requirements - part 11: Wireless lan medium access control (mac) and physical layer (phy) specifications. *IEEE Std 802.11-2016 (Revision of IEEE Std 802.11-2012)* (2016), 1–3534.

[3] Ieee standard for local and metropolitan area networks–part 15.7: Short-range wireless optical communication using visible light. *IEEE Std 802.15.7™-2018* (2018), 1–405.

[4] Ab-Rahman, M. S., Shuhaimi, N. I., Azizan, L. A.-H., and Hassan, M. R. Analytical study of signal-to-noise ratio for visible light communication by using single source. *Journal of Computer Science*, 1 (Nov. 2011), 141–144.

[5] Ageev, A., Luci, E., Petrioli, C., and Thakker, N. Vulcan: A low-cost, low-power embedded visible light communication and networking platform. In *Proceedings of the 22nd International ACM Conference on Modeling, Analysis and Simulation of Wireless and Mobile Systems* (New York, NY, USA, 2019), MSWIM '19, Association for Computing Machinery, p. 127–134.

[6] Aldalbahi, A., Rahaim, M., Khreishah, A., Ayyash, M., and Little, T. D. C. Visible light communication module: An open source extension to

the ns3 network simulator with real system validation. *IEEE Access 5* (2017), 22144–22158.

[7] Basnayaka, D. A., and Haas, H. Hybrid rf and vlc systems: Improving user data rate performance of vlc systems. In *Proceedings of IEEE VTC* (May 2015), IEEE, pp. 1–5.

[8] Bazan, O., and Jaseemuddin, M. On the design of opportunistic mac protocols for multihop wireless ; networks with beamforming antennas. *IEEE Transactions on Mobile Computing 10*, 3 (2011), 305–319.

[9] Benedetti, D., Petrioli, C., and Spenza, D. Greencastalia: An energy-harvesting-enabled framework for the castalia simulator. In *Proceedings of the 1st International Workshop on Energy Neutral Sensing Systems* (New York, NY, USA, 2013), ENSSys '13, Association for Computing Machinery.

[10] Bouchet, O., Porcon, P., Wolf, M., Grobe, L., Walewski, J. W., Nerreter, S., Langer, K., Fernández, L., Vucic, J., Kamalakis, T., Ntogari, G., and Gueutier, E. Visible-light communication system enabling 73 mb/s data streaming. In *2010 IEEE Globecom Workshops* (2010), pp. 1042–1046.

[11] Boulis, A., et al. Castalia: A simulator for wireless sensor networks and body area networks. *NICTA: National ICT Australia 83* (2011).

[12] Bykhovsky, D., and Arnon, S. Multiple access resource allocation in visible light communication systems. *Journal of Lightwave Technology 32*, 8 (2014), 1594–1600.

[13] Cai, H., and Wolf, T. On 2-way neighbor discovery in wireless networks with directional antennas. In *2015 IEEE Conference on Computer Communications (INFOCOM)* (2015), pp. 702–710.

[14] Candy, J. *CHIRP-Like Signals: Estimation, Detection and Processing A Sequential Model-Based Approach.* Lawrence Livermore National Laboratory, Department of Energy, United States, 2016.

[15] Cen, N., Dave, N., Demirors, E., Guan, Z., and Melodia, T. Libeam: Throughput-optimal cooperative beamforming for indoor visible light networks. In *IEEE INFOCOM 2019-IEEE Conference on Computer Communications* (2019), IEEE, pp. 1972–1980.

[16] Cen, N., Jagannath, J., Moretti, S., Guan, Z., and Melodia, T. Lanet: Visible-light ad hoc networks. *Ad Hoc Networks 84* (March 2019), 107–123.

[17] Chang, F., Hu, W., Lee, D., and Yu, C. Design and implementation of anti low-frequency noise in visible light communications. In *Proceedings of ICASI* (May 2017), pp. 1536–1538.

[18] Chang He, Lie-liang Yang, Pei Xiao, and Imran, M. A. Ds-cdma assisted visible light communications systems. In *2015 IEEE 20th International Workshop on Computer Aided Modelling and Design of Communication Links and Networks (CAMAD)* (2015), pp. 27–32.

[19] Chen, C., Ijaz, M., Tsonev, D., and Haas, H. Analysis of downlink transmission in dco-ofdm-based optical attocell networks. In *2014 IEEE Global Communications Conference* (2014), pp. 2072–2077.

[20] Chen, S., and Chow, C. Color-shift keying and code-division multiple-access transmission for rgb-led visible light communications using mobile phone camera. *IEEE Photonics Journal 6*, 6 (2014), 1–6.

[21] Choudhury, R. R., and Vaidya, N. H. Deafness: a mac problem in ad hoc networks when using directional antennas. In *Proceedings of the 12th IEEE International Conference on Network Protocols, 2004. ICNP 2004.* (2004), pp. 283–292.

[22] Chow, C., Yeh, C., Liu, Y., and Liu, Y. Digital signal processing for light emitting diode based visible light communication. *IEEE Photon. Soc. Newsletter* (October 2012), 9–13.

[23] Cisco. Annual internet report (2018–2023) white paper. Tech. rep., 2020.

[24] Costanzo, A., Loscri', V., and Costanzo, S. Adaptive dual color visible light communication (VLC) system. *Trends and Advances in Information Systems and Technologies 746* (May 2018), 1478–1487.

[25] Dang, J., and Zhang, Z. Comparison of optical ofdm-idma and optical ofdma for uplink visible light communications. In *2012 International Conference on Wireless Communications and Signal Processing (WCSP)* (2012), pp. 1–6.

[26] Datta, K. N., Das, P., Saha, M., Saha, S., and Chakraborty, S. Exploring visible light communication system using rts/cts mechanism for mobile environment. In *Proceedings of the 24th Annual International Conference on Mobile Computing and Networking* (New York, NY, USA, 2018), MobiCom '18, Association for Computing Machinery, p. 732–734.

[27] Duque, A., Stanica, R., Rivano, H., and Desportes, A. Unleashing the power of LED-to-camera communications for IoT devices. In *Proceedings of ACM Workshop on Visible Light Communication Systems* (2016), ACM, pp. 55–60.

[28] Duque, A., Stanica, R., Rivano, H., and Desportes, A. CamComSim: a LED-to-Camera Communication Simulator. Research Report RR-9114, INSA Lyon ; INRIA Grenoble - Rhône-Alpes ; CITI - CITI Centre of Innovation in Telecommunications and Integration of services ; Rtone, Oct. 2017.

[29] Felemban, E., Murawski, R., Ekici, E., Park, S., Lee, K., Park, J., and Mir, Z. Sand: Sectored-antenna neighbor discovery protocol for wireless networks. pp. 82–90.

[30] Fokas, M., Katsianis, D., Varoutas, D., Rokkas, T., Javaudin, J., Bellec, M., Goni, G., and Gonzalez Fuentetaja, R. Initial techno-economic results for omega home gigabit networks. In *21st Annual IEEE International Symposium on Personal, Indoor and Mobile Radio Communications* (2010), pp. 2793–2798.

[31] Galisteo, A., Juara, D., and Giustiniano, D. Research in visible light communication systems with OpenVLC1.3. In *In Proceedings of IEEE WF-IOT* (2019), IEEE.

[32] Garcia-Retegui, R., Gonzalez, S. A., Funes, M. A., and Maestri, S. Implementation of a novel synchronization method using Sliding Goertzel DFT. In *Proceedings of IEEE International Symposium on Intelligent Signal Processing* (October 2007), IEEE, pp. 1–5.

[33] Ghimire, B., and Haas, H. Resource allocation in optical wireless networks. In *2011 IEEE 22nd International Symposium on Personal, Indoor and Mobile Radio Communications* (2011), pp. 1061–1065.

[34] Haas, H., Yin, L., Wang, Y., and Chen, C. What is LiFi? *Journal of Lightwave Technology 34*, 6 (March 2016), 1533–1544.

[35] Haykin, S. *Communication Systems.* Wiley Publishing, 2009.

[36] Heydariaan, M., Yin, S., Gnawali, O., Puccinelli, D., and Giustiniano, D. Embedded visible light communication: Link measurements and interpretation. In *Proceedings of EWSN* (2016), Junction Publishing, pp. 341–346.

[37] Hranilovic, S. *Wireless Optical Communication Systems.* Springer-Verlag, 2009.

[38] Jagannath, J., and Melodia, T. An opportunistic medium access control protocol for visible light ad hoc networks. In *2018 International Conference on Computing, Networking and Communications (ICNC)* (March 2018), pp. 609–614.

[39] Kahn, J. M., and Barry, J. R. Wireless infrared communications. *Proceedings of the IEEE 85*, 2 (1997), 265–298.

[40] Kay, S. *Fundamentals of statistical signal processing.* Prentice Hall PTR, 1993.

[41] Klaver, L., and Zuniga, M. Shine : A step towards distributed multi-hop visible light communication. In *Proceedings of IEEE MASS* (Oct 2015), IEEE, pp. 235–243.

[42] Komine, T., and Nakagawa, M. Fundamental analysis for visible-light communication system using led lights. *IEEE Transactions on Consumer Electronics 50*, 1 (2004), 100–107.

[43] Korakis, T., Jakllari, G., and Tassiulas, L. Cdr-mac: A protocol for full exploitation of directional antennas in ad hoc wireless networks. *IEEE Transactions on Mobile Computing 7*, 2 (2008), 145–155.

[44] Ley-Bosch, C., Alonso-González, I., Sanchez-Rodriguez, D., and Ramírez-Casañas, C. Evaluation of the effects of hidden node problems in ieee 802.15.7 uplink performance. *Sensors 16* (02 2016), 216.

[45] Ley-Bosch, C., Medina-Sosa, R., Alonso-González, I., and Sánchez-Rodríguez, D. Implementing an ieee802.15.7 physical layer simulation model with omnet++. In *Distributed Computing and Artificial Intelligence, 12th International Conference* (Cham, 2015), Springer International Publishing, pp. 251–258.

[46] Li, L., Hu, P., Peng, C., Shen, G., and Zhao, F. Epsilon: A visible light based positioning system. In *USENIX Symposium on NSDI* (April 2014), USENIX Association, pp. 331–343.

[47] Li, S., Pandharipande, A., and Willems, F. M. J. Two-way visible light communication and illumination with LEDs. *IEEE Transactions on Communications 65*, 2 (Feb 2017), 740–750.

[48] Lin, P., and Zhang, L. Full-duplex RTS/CTS aided CSMA/CA mechanism for visible light communication network with hidden nodes under saturated traffic. In *2018 IEEE International Conference on Communications, ICC 2018, Kansas City, MO, USA, May 20-24, 2018* (2018), IEEE, pp. 1–6.

[49] Liu, C., Jin, X., Zhu, W., Jin, M., and Xu, Z. Demonstration of a low complexity ARM-based indoor VLC transceiver under strong interference. In *Proceedings of IWCMC* (June 2017), IEEE, pp. 622–627.

[50] Martin-Gonzalez, J. A., Poves, E., and Lopez-Hernandez, F. J. Random optical codes used in optical networks. *IET Communications 3*, 8 (2009), 1392–1401.

[51] Microelectronics, S. Stm32, arm cortex- m 7 nucleo-144 development board.

[52] Miramirkhani, F., and Uysal, M. Channel modeling and characterization for visible light communications. *IEEE Photonics Journal 7*, 6 (2015), 1–16.

[53] Mould, R. F. Thomas edison (1847–1931). biography with special reference to x-rays. *Nowotwory. Journal of Oncology 66*, 6 (2016), 499–507.

[54] Musa, A., Baba, M. D., and Haji Mansor, H. M. A. The design and implementation of ieee 802.15.7 module with ns-2 simulator. In *2014 International Conference on Computer, Communications, and Control Technology (I4CT)* (2014), pp. 111–115.

[55] Nam-Tuan Le, and Yeong Min Jang. Broadcasting mac protocol for ieee 802.15.7 visible light communication. In *2013 Fifth International Conference on Ubiquitous and Future Networks (ICUFN)* (2013), pp. 667–671.

[56] Nur, F., Habib, M. A., Razzaque, A., Islam, M., Almogren, A., Hassan, M., and Alamri, A. Collaborative neighbor discovery in directional wireless sensor networks: algorithm and analysis. *EURASIP Journal on Wireless Communications and Networking 2017* (12 2017).

[57] Pathak, P. H., Feng, X., Hu, P., and Mohapatra, P. Visible Light Communication, Networking, and Sensing: A Survey, Potential and Challenges. *IEEE Communications Surveys Tutorials 17*, 4 (2015), 2047–2077.

[58] Prashanth, L., Kattapagari, K., Chitturi, R., Baddam, V., and Prasad, L. A review on role of essential trace elements in health and disease. *Journal of Dr. NTR University of Health Sciences 4*, 2 (2015), 75–85.

[59] Proakis, J. G., and Manolakis, D. K. *Digital Signal Processing.* Prentice-Hall, Inc., NJ,USA, 2006.

[60] Rahaim, M. B., Borogovac, T., and Carruthers, J. B. Candles: Communication and lighting emulation software. In *Proceedings of the Fifth ACM International Workshop on Wireless Network Testbeds, Experimental Evaluation and Characterization* (New York, NY, USA, 2010), WiNTECH '10, Association for Computing Machinery, p. 9–14.

[61] Schmid, S., Bourchas, T., Mangold, S., and Gross, T. Linux Light Bulbs: Enabling internet protocol connectivity for light bulb networks. In *Proceedings of the International Workshop on Visible Light Communications Systems* (2015), ACM, pp. 3–8.

[62] Schmid, S., Corbellini, G., Mangold, S., and Gross, T. LED-to-LED visible light communication networks. In *Proceedings of ACM MobiHoc* (2013), ACM, pp. 1–10.

[63] Schmid, S., von Deschwanden, B., Mangold, S., and Gross, T. R. Adaptive software-defined visible light communication networks. In *Proceedings of IEEE/ACM IoTDI* (2017), IEEE, pp. 109–120.

[64] Shoreh, M. H., Fallahpour, A., and Salehi, J. A. Design concepts and performance analysis of multicarrier cdma for indoor visible light communications. *IEEE/OSA Journal of Optical Communications and Networking 7*, 6 (2015), 554–562.

[65] Sliney, D. What is light? the visible spectrum and beyond. *Eye 30*, 2 (2016), 222–229.

[66] Tagliaferri, D., and Capsoni, C. Development and testing of an indoor vlc simulator. In *2015 4th International Workshop on Optical Wireless Communications (IWOW)* (2015), pp. 122–126.

[67] Tanaka, Y., Haruyama, S., and Nakagawa, M. Wireless optical trasnsmissions with white colored led for wireless home links. pp. 1325–1329. 11th IEEE International Symposium on Personal, Indoor and Mobile Radio Communications (PIMRC 2000) ; Conference date: 18-09-2000 Through 21-09-2000.

[68] Tian, Z., Wright, K., and Zhou, X. The Darklight Rises: Visible light communication in the Dark: Demo. In *In Proceedings of ACM MobiCom* (New York City, New York, October 2016), ACM, pp. 495–496.

[69] Tobagi, F., and Kleinrock, L. Packet switching in radio channels: Part ii - the hidden terminal problem in carrier sense multiple-access and the busy-tone solution. *IEEE Transactions on Communications 23*, 12 (December 1975), 1417–1433.

[70] Tsonev, D., Videv, S., and Haas, H. Towards a 100 Gb/s visible light wireless access network. *Optics Express 23*, 2 (Jan 2015), 1627–1637.

[71] Varga, A., and Hornig, R. An overview of the omnet++ simulation environment. Simutools '08, ICST (Institute for Computer Sciences, Social-Informatics and Telecommunications Engineering).

[72] Vasudevan, S., Kurose, J., and Towsley, D. On neighbor discovery in wireless networks with directional antennas. In *Proceedings IEEE 24th Annual Joint Conference of the IEEE Computer and Communications Societies.* (2005), vol. 4, pp. 2502–2512 vol. 4.

[73] Wang, Q., and Giustiniano, D. Intra-frame bidirectional transmission in networks of visible leds. *IEEE/ACM Transactions on Networking 24*, 6 (December 2016), 3607–3619.

[74] Wang, Q., Giustiniano, D., and Puccinelli, D. An open source research platform for embedded visible light networking. *IEEE Wireless Communications 22*, 2 (April 2015), 94–100.

[75] Wang, Q., Giustiniano, D., and Zuniga, M. In light and in darkness, in motion and in stillness: A reliable and adaptive receiver for the internet of lights. *IEEE Journal on Selected Areas in Communications 36*, 1 (2018), 149–161.

[76] Wang, Z., Liu, Y., Lin, Y., and Huang, S. Full-duplex mac protocol based on adaptive contention window for visible light communication. *J. Opt. Commun. Netw. 7*, 3 (Mar 2015), 164–171.

[77] Wu, Z., and Little, T. *IET Communications 6* (March 2012), 525–531(6).

[78] Yam, F., and Hassan, Z. Innovative advances in led technology. *Microelectronics Journal 36*, 2 (2005), 129–137.

[79] Yin, S., and Gnawali, O. Towards embedded visible light communication robust to dynamic ambient light. In *Proceedings of IEEE GLOBECOM* (Dec 2016), IEEE, pp. 1–6.

[80] Yin, S., Smaoui, N., Heydariaan, M., and Gnawali, O. Purple VLC: Accelerating visible light communication in room-area through PRU offloading. In *Proceedings of ACM EWSN* (Madrid, Spain, 2018), pp. Madrid, Spain, 67–78.

[81] Young-Bae Ko, Shankarkumar, V., and Vaidya, N. H. Medium access control protocols using directional antennas in ad hoc networks. In *Proceedings IEEE INFOCOM 2000. Conference on Computer Communications. Nineteenth Annual Joint Conference of the IEEE Computer and Communications Societies (Cat. No.00CH37064)* (March 2000), vol. 1, pp. 13–21 vol.1.

[82] Zhao, Y., and Vongkulbhisal, J. Design of visible light communication receiver for on-off keying modulation by adaptive minimum-voltage cancelation. *Engineering Journal 17*, 4 (June 2013), 125–129.